LUND INSTITUTE OF TECHNOLOGY
Lund University

Active Biotech

Expression and Purification of Recombinant Human S100A8 and S100A9 for Characterization of Their Roles as Danger Signals

By Rebecca Trang

Submitted in partial fulfilment of the requirements for the degree of
Master of Science in Biotechnology

June 2015

Supervisors: Helén Carlsson-Nyhlén, Ph. D. and Leif Dahlberg, Ph. D. at Active Biotech AB; Johan Svensson Bonde, Ph. D. at Lund University.
Examiner: Professor Leif Bülow, Department of Applied Biochemistry, Lund University

Abstract

The direct involvement of S100 calcium-binding proteins A8 (S100A8) and A9 (S100A9) in numerous human diseases have been discovered more than 20 years ago, and they have ever since emerged as a very potent biomarker. Increased levels of S100A8 and S100A9 have been found in inflammation and various cancers. As complexes, they become crucial danger signals and act as endogenous activators of TLR4 (Toll-like receptor 4) and RAGE (Receptor for Advanced Glycation Endoproducts) on sentinel cells. As danger signals, they activate TLR4- and RAGE-dependent signaling cascades, especially the NF-κB (Nuclear Factor kappa-light-chain-enhancer of activated B cells) signalling pathway.

S100A8 and S100A9 have become the focus of many current researches since they seem to play a central role as danger signals, however the initial events during binding of the proteins to their receptors remain questionable. The aim of this project was to produce recombinant human S100A8 (rhS100A8) and recombinant human S100A8/S100A9 (rhS100A8/S100A9) to characterize their role as ligands of TLR4-MD2 and RAGE *in vitro* with surface plasmon resonance (SPR) and as activators of the NF-κB cell-signalling pathway in cell-based *in vitro* system with NF-κB Luciferase reporter assay.

Within the scope of producing rhS00A8, the protein was expressed in its wild-type (wt) form and compared to S100A8 fused to a His_6-tag (His_6-rhS100A8). The study observed a much lower stability of wt-rhS100A8, with degradation when subject to potential oxidation. Characterization of His_6-S100A8 and wt-rhS100A8/S100A9 confirmed: i) *in vitro* binding activities of His_6-S100A8 to TLR4-MD2 and RAGE with SPR studies; ii) cell-based *in vitro* binding activities of wt-rhS100A8/S100A9 to TLR4 with NF-κB Luciferase reporter assay and iii) lower binding activities of heterocomplex compared to homocomplex in both previously mentioned systems.

Acknowledgement

The project presented in this master's thesis was performed at Active Biotech Bioscience department, in Lund, Sweden from January to June 2015.

This project consumed huge amounts of interdisciplinary lab work and it would not be possible if I did not have the support of many individuals at Active Biotech. Therefore, I would like to extend my sincere gratitude to all of them.

First of all, I am very thankful to David Liberg and my supervisors Helén Carlsson-Nyhlén and Leif Dahlberg for giving me this opportunity to carry out my master's project at Active Biotech and to experience what science is about outside of academia. I would like to express my gratitude to both Helén Carlsson-Nyhlén and Leif Dahlberg for the helpful guidance and the extra work they have volunteered to help me complete my experiments and in reviewing this thesis. I am thankful for a great company both on a personal and on a professional level, and for the encouragements that have helped me complete my thesis.

I would also like to express my warm thanks to Per Björk for sharing his wisdom and expertise. Lastly, I would like to show my gratitude to Per Björk, Mats Nilsson and Anneli Nilsson who devoted their time and knowledge in supporting me in my experiments.

Table of Contents

Chapter 1

Introduction and Project Aims

The project presented in this master's thesis was brought together by Active Biotech AB, Lund, Sweden.

Active Biotech is a company focusing on research and development of pharmaceuticals for treatments of cancer and inflammatory disease. One of their on-going projects is a pre-clinical project called the ISI project, which focuses on development of small inhibitory molecules. These small inhibitory molecules will act upon interactions between S100 proteins and their ligands – interactions that are involved in many human diseases. Within the ISI project, S100 proteins are produced and used as reagents for research purposes in order to learn more about them and their role in human diseases.

Up until recently, the ISI project has been producing and studied several members of the S100 protein family, including S100A9. *In vivo*, S100A9 can exist with another member, the S100A8, and they both can exist as both homo- and heterodimers. Both proteins have emerged as important pro-inflammatory mediators in acute and chronic inflammation, and increased levels of both proteins have also been detected in various human cancers. Although recent studies have proposed many different functions of the complex, the molecular mechanism still remains to be defined. For the sake of the ISI project, it is therefore of interest to produce and study S100A8 and S100A8/S100A9 heterodimer complex. Active Biotech saw the opportunity to include some parts of the project into a master's project.

There are four aims of this master's project:

i. To investigate commercially available vectors and use the most suitable one to express and purify functional recombinant human S100A8 (rhS100A8) fused to an affinity tag, and possibly remove the tag after.
ii. To study tagged rhS100A8 and compare with wild-type rhS100A8 (wt-rhS100A8) in terms of expression in *Escherichia coli*, purification and final product yield.
iii. To express and purify wt-rhS100A9 and wt-rhS100A8 in order to form heterodimer complexes.
iv. To study and compare the expressed proteins using chemical and biochemical analyses as well as in a cell-based system.

Chapter 2

Background of Human S100A8 and S100A9

The main focus of this chapter is to briefly introduce the reader to the proteins that have the main roles of this master's project. These proteins became the focus of many current researches due to their association with numerous human diseases where they play a central role in many biological processes, both intra- and extracellular. This chapter will highlight some of their interesting features and functions, their physical appearance and their biological role. The chapter will finish off with a brief introduction to the parts of cell biology that are central to these proteins.

2.1 Protein Structure

S100A8 and S100A9 are members of the family of low molecular weight S100 proteins, found only in vertebrates. S100A8 is a 10.8 kDa protein with 93 amino acids and S100A9 is a 13.1 kDa protein with 113 amino acids. Both are structurally characterized by two EF-hand calcium-binding regions – one with high affinity and the other one with low affinity to Ca^{2+}. The two calcium-binding regions are located in two separate loops. Each loop is positioned between two supporting α-helices. *In vivo*, they have the tendency to form non-covalent and antiparallel associated complexes (as reviewed in Goyette and Geczy, 2011), either as homodimers (S100A8/S100A8 and S100A9/S100A9) or heterodimers (S100A8/S100A9), with the latter being the most predominantly occurring form with higher stability (Vogl, 2010). They are surprisingly much dependent on one another's existence, that deleting an S100A9 gene (in mice model) lead to the absence of S100A8 at protein level (Manitz *et al*., 2003). A schematic overview with aligned amino-acid sequences can be viewed in *Figure 2.1*, and the tertiary and quaternary structure of the dimers can be seen in *Figure 2.2*.

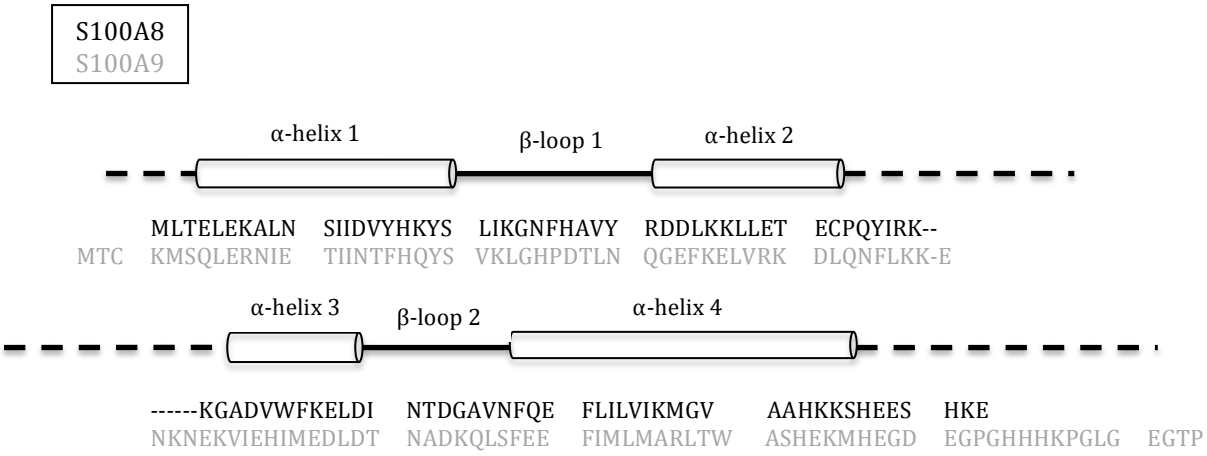

Figure 2.1. Schematic overview with highlighted α-helices, Ca^{2+}-binding β-loops and the aligned amino-acid sequences of human S100A8 and S100A9 (adapted from Ishikawa *et al.*, 2000).

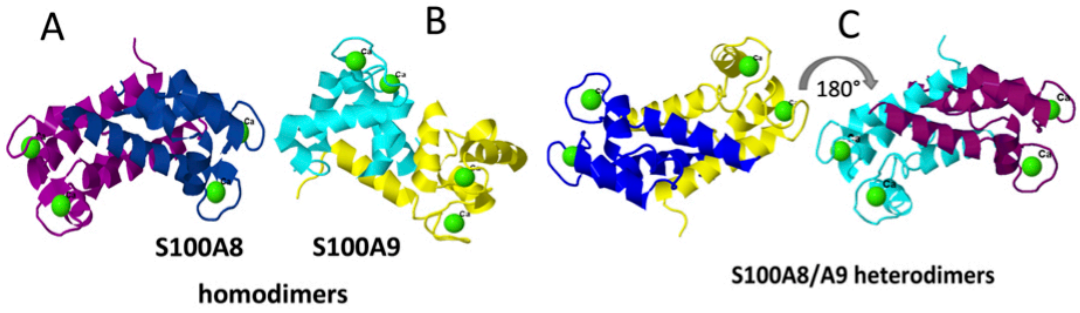

Figure 2.2. Tertiary and quaternary structures of S100A8 and S100A9. (**A**) and (**B**) show homodimers; individual subunit are shown in colours –purple and dark blue for S100A8 and sea-blue and yellow for S100A9. (**C**) shows a S100A8/S100A9 heterodimer in two projections rotated by 180° (adapted from Vogl *et al.*, 2012).

Since both proteins have high affinity to Ca^{2+}, the ions drastically modulate the stability of the proteins by increasing the thermal stability of homo- and heterodimers, as well as triggering conformational movements (as reviewed in Vogl *et al.*, 2012). The conformational movements allow S100A8 and S100A9 to interact with each other (to form dimers) or with other proteins. Apart from having affinity to Ca^{2+}, both proteins also have affinity to other bivalent ions, including Zn^{2+}. In the presence of both ions, the heterodimers can also assemble into heterotetrameric and even larger complexes in a Ca^{2+} and Zn^{2+}-dependent manner (Korndörfer *et al.*, 2007; Leukert *et al.*, 2006; Strupat *et al.*, 2000).

2.2 Functionality and Clinical Occurrence

S100A8 and S100A9 are expressed in cells of myeloid origin, such as phagocytes, and are abundant in the cytosol. Especially in neutrophils and monocytes (types of phagocytes) these proteins constitute up to 45% of neutrophil cytosolic

protein and 1% in monocyte (as reviewed in Hessian *et al*., 1993). In steady-state conditions, they are expressed to regulate cell homeostasis, interacting especially with cytoskeletons (as reviewed in Ehrchen *et al*., 2009). However, when phagocytes are activated by stress responses, both proteins are secreted to the extracellular compartment by a non-classical secretory pathway (Rammes *et al*., 1997). Under inflammatory conditions, the expressions of S100A8 and S100A9 are also up-regulated by keratinocytes and epithelial cells in response to stress (Mørk *et al*., 2003; Ross and Herzberg, 2001). Increased levels of S100A8 and S100A9 have shown to exhibit pro-inflammatory activities in many inflammatory human diseases (*Table 2.1*). This association has been discovered more than 20 years ago and they have ever since emerged as a very potent biomarker.

In cancer progression, the intracellular S100A8/S100A9 heterodimer complex has tumour-promoting activities (Ichikawa *et al.*, 2011) where they regulate the accumulation of myeloid-derived cells (Cheng *et al*., 2008; Sinha *et al.*, 2008;). This suggests the expansion of immature myeloid cell population during inflammation and in tumour (Gabrilovich and Nagaraj, 2009). The myeloid cells act as potent suppressors of T-mediated immune responses, inhibiting the dendritic cell differentiation and suppressing antitumor immune responses. These are some of the main immunological abnormalities in cancer. In addition, high levels of S100A8 and S100A9 have been found in various cancers, such as breast, lung, gastric, pancreatic and prostate cancer (Arai *et al*., 2001; El-Rifai *et al*., 2002; Shen *et al*., 2004; Cross *et al*., 2005; Carlsson *et al*., 2005; Hermani *et al*., 2005).

Table 1.1. Associations of S100A8/S100A9 and human diseases (adapted from Ehrchen *et al*., 2009)

Conditions
Rheumatoid arthritis
Juvenile idiopathic arthritis
Psoriatic arthritis
Sepsis
Atherosclerosis
Acute coronary syndrome/Myocardial infraction
Diabetes
Psoriasis/Inflammatory skin disease
Inflammatory bowel disease
Vasculitis
Transplant rejection
Systemic Lupus Erythematosus/Glomerulonephritis
Pancreatitis
Cancer
Dermatomyositis/polymyositis
Hyperzincemia/systemic inflammation

In inflammation, both proteins are secreted to the extracellular compartment by a non-classical secretory pathway (Rammes *et al*., 1997). Once secreted, they play a critical role in the pathogenesis of inflammatory disorders. As a heterodimer complex, they become crucial danger signals during inflammatory processes in infection, autoimmunity and also cancer, referred to as DAMPs (danger/damage-associated molecular pattern). The heterodimer complexes are recognized by sentinel cells (danger-sensing cells) by acting as endogenous activators of TLR4 (Toll-Like Receptor 4) (Vogl *et al*., 2007; Loser *et al.*, 2010) and RAGE (Receptor for Advanced Glycation Endoproducts) (Narumi *et al*., 2015), promoting inflammatory processes in infections and autoimmunity. One of the consequences of activating TRL4 and RAGE is the production of pro-inflammatory cytokines, chemokines and reactive oxygen species (ROS) (Lim *et al*., 2011; reviewed in Medzhitov and Janeway, 2002). ROS are normally generated in low levels to mediate numerous cell-signalling pathways, however when excessively generated, such as during inflammation, they can damage tissues and produce several oxidation products that can lead to chronic inflammation (as reviewed in Kunsch and Medford, 1999). It is suggested that S100A9 and especially S100A8 can also act as oxidant scavengers under inflammatory responses to protect tissue against oxidative damages, thus they are also susceptible to oxidative modifications by various forms of ROS (Lim *et al*., 2011). Lim *et al.* (2011) also propose that the oxidative modifications can alter the proteins' function, their structure or generate adducts. It is also known that proteins that are target of free radicals are subject to fragmentation and denaturation (as reviewed in Bourdon and Blache, 2001).

2.3 Cell Biology

As endogenous danger signal, DAMPs such as S100A8/S100A9s, promote and aggravate the inflammatory responses by activating cell types of the innate immune system. Activation is initiated once DAMPs interacts with DAMP receptors positioned on the cell membranes, such as TLRs or RAGE, leading to amplified inflammatory reactions (as reviewed in Bianchi, 2007). Since they possess cytokine-like and chemokine-like activities, S100A8 and S100A9 are able to activate RAGE- and TLR4-dependent signalling cascades, especially the NF-κB (Nuclear Factor kappa-light-chain-enhancer of activated B cells) signalling pathway (Simard *et al.,* 2013), and potentially other signalling pathways as well (Vogl *et al.*, 2004).

2.3.1 NF-κB Signalling Pathway

NF-κB (Nuclear Factor kappa-light-chain-enhancer of activated B cells) is a protein complex transcription factor found in almost all animal cell types. NF-κB is involved in the pro-inflammatory signalling pathway and regulates important physiological processes including immune response to infection, inflammation, cell growth, apoptosis and tumorigenesis (as reviewed in Egan and Toruner, 2006). Due to its central role, particularly in models of inflammation and cancer, the NF-κB signalling pathway has become target for pharmacological intervention.

In most cells, NF-κB is present as latent and inactive in the cytoplasm. Many different stimuli/inducers have been identified to activate the NF-κB pathway through extracellular signals via receptors. The inducers include "pro-inflammatory cytokines, pathogenic bacteria and viruses, bacterial lipopolysaccharides, peptidoglycan and oxidative stress" (Egan and Toruner, 2006). Following the activation, NF-κB rapidly enters the nucleus and controls the transcription of DNA by binding to a NF-κB response element (short sequences of DNA within the gene promoter region that are able to bind NF-κB). They activate the expression of pro-inflammatory genes including cytokines and adhesion molecules (as reviewed in Lawrence, 2009) in a cascade-manner (i.e. cytokines activate the NF-κB and stimulate their target cells to express additional cytokines). Some types of cytokines bind to their respective receptor on immune cells and can affect the cells' behaviour as well as the interaction and communication between the cells. Other types of cytokines provoke the inflammatory responses (Zhang and An, 2007).

2.3.2 TLR4/TLR4-MD2

Toll-like-receptor 4 (TLR4) is part of the Toll-like receptor family and a type of pattern recognition receptor (PRR) (as reviewed in Lawrence, 2009). TLR4 plays

a significant role in pathogen recognition and activation of the innate immunity. Expressed in varies tissues and cell types, its role is to respond to invading pathogen-associated molecular patterns (PAMPs) and endogenous damage/danger-associated molecular patterns (DAMPs) in the early innate immune response (as reviewed in Bianchi, 2007). Lipopolysaccharides (LPS), or endotoxins, from Gram-negative bacteria are prototypical PAMPs, specifically recognized by TLR4 (as reviewed in Medzhitov and Janeway, 2002) in complex with another protein known as MD2. When TLR4-MD2 recognizes LPS, it induces the release of critical pro-inflammatory mediators, which in turn are necessary to activate potent immune responses. A major hallmark of the LPS response is the activation of the transcription factor NF-κB.

Apart from PAMPs, endogenous DAMPs also trigger TLR4 during tissue injury and certain disease states. Although structurally different, they also promote inflammation by initiating signalling cascades leading to activation of transcription factors including NF-κB (as reviewed in Bianchi, 2007). Studies have shown that S100A8/S100A9 complexes are endogenous activators of TLR4 (Kang *et al*., 2015; Vogl *et al*., 2007; Loser *et al.*, 2010), hence they are considered as DAMPs. In addition, Vogl *et al*. (2007) provided the first evidence that purified S100A8 specifically bound to TLR4-MD2 complex.

2.3.3 RAGE

Receptor for Advanced Glycation Endoproduct (RAGE) is a multiligand receptor belonging to the immunoglobulin (Ig) superfamily. They are expressed at low levels under normal physiological conditions in the majority of tissues (as reviewed in Buckley and Ehrhardt, 2009), however they are highly up-regulated in sites of inflammation and oxidative stress, largely in inflammatory cells such as macrophages and epithelial cells (as reviewed in Sparvero *et al*., 2009). In cancer they are also expressed in various tumour cells (Yamagishi et al., 2015).

RAGE receptors have the ability to bind to AGE (Advanced Glycation Endoproducts), a product that is formed during aging and accelerated under pathophysiologic states. Apart from AGE, RAGE also binds endogenous ligands generated by cell death and tissue injuries, including amyloid β-peptide, S100/calgranulin family proteins, high mobility group B1 (HMGB1, also known as amphoterin) and leukocyte integrins. Stimulations of RAGE induce the activation of the NF-κB pathway (van Beijnum *et al.*, 2007). Studies have shown that S100A8/S100A9 complexes bind to RAGE (Kang *et al*., 2015; Hermani *et al*., 2006; Ghavami *et al*., 2008; Boyd et al., 2008) and promoted activation of NF-κB (Kang *et al*., 2015; Hermani *et al*., 2006; Ghavami *et al*., 2008).

Chapter 3

Choice of Vector for the Expression of Recombinant Human S100A8 Fused to a Tag

In theory, producing a recombinant protein is very straightforward. Clone the gene of interest in an expression vector, transform it into a host cell, cultivate the cells, induce, and the protein production has begun. The proteins are then ready to be extracted, purified and characterized. In reality, the challenges could be to not obtain any proteins at all, poor growth or non-functional proteins, to name a few. What is also confusing are the dozens of choices that needs to be made along the way to come up with a strategy to produce the target protein.

The most central part of this project was to express recombinant human S100A8 fused to a tag. This section describes the methodology used to find a suitable vector, initiating with evaluations of commercially available vectors followed by choosing a method for cleavage.

3.1 Choice of Affinity Tag

Purified proteins are often obtained in a recombinant form, optimally with an affinity/fusion tag added to the protein by recombinant DNA technology. The use of a tag is known to be advantageous in terms of: i) facilitating purification from the *E. coli* cellular milieu where one-step purification can even be achieved; ii) achieving higher solubility by using larger tag; iii) being removed to produce wild-type protein, where the removal can be both easy and specific; iv) having minimal effect on tertiary structure and biological activity if using small tags (reviewed in Terpe, 2002).

The project started off with an investigation of a variety of affinity tags. Since one of the project aims was to study the recombinant protein with and without its tag, the investigation continued to restrict to small peptide tags only. This is due to the fact that fusion proteins are too big in size and would interfere with the structure and biochemical activity of the recombinant protein if left uncleaved. Small peptide tags have the advantages of being less likely to interfere with the fused protein and they usually allow for single-step purification with resins that can specifically and strongly bind to the tags.

The candidates for the choice of affinity tags were the smallest, commercially available ones. These were poly-Arg, poly-His, FLAG and Strep-II. The first elimination stage was based on ease of removal. The poly-Arg was eliminated with reason that it is limited by poor cleavage yields and unwanted cleavage within desired protein sequence (Nagai and Thogersen, 1987). In addition, they are not used very often. FLAG was also eliminated with reason that the system uses monoclonal-antibody purification matrix, which is not stable compared to the others (Ni^{2+}/Zn^{2+}/Co^{2+} or Strep-Tactin) (Terpe, 2002). The high resin cost is also one of its disadvantages. Seeing as Strep-II and poly-His tag are equally good, the final elimination stage was based on published data and the occurrence of commercially available tagged S100A8. The choice of tag was the poly-His tag with six histidine in tandem. Despite the fact that poly-His tags are rumored to provoke negative effects on the tertiary structure or biological activity (Wu and Filutowicz, 1999; Klose *et al.*, 2004; Chant *et al.*, 2005; Khan *et al.*, 2012), there are published data of successful production of recombinant His-tagged S100A8 (Ryckman *et al.*, 2003; Qin *et al.*, 2010). There are also commercially available His-tagged hS100A8s that can be purchased from Life Technologies (a Thermo Fisher Scientific brand) and Sino Biologicals, to name a few.

Affinity tags can be positioned either at the N-terminal or C-terminal of the recombinant protein. Which end-terminal to choose from is much dependent on the three-dimensional structure of the recombinant protein (as reviewed in Rosano and Ceccarelli, 2014). In the study conducted by Ryckman et al., 2003 they approached with the tag fused to the N-terminus of hS100A8. In addition, the commercially available hS100A8 also had the His-tag fused to its N-terminus. Knowing of this, fusing it to the N-terminus was also the approach for this project.

3.2 Choice of Enzymatic Cleavage

After a suitable tag was chosen, the next phase was to find an enzymatic cleavage strategy that would enable a clean cut, i.e. the recombinant protein is left with no extraneous amino acids. An investigation was carried out to find a commercially available expression vector system, which could offer different options on protease recognition sites for enzymatic cleavage. Based on previous in-house experiments, pET vector systems provided by Novagen are both reliable and good expression vectors. In addition, they are also suitable to be transformed into *E. coli* BL21(DE3), which is the choice of host cells. The pET systems offers three different protease recognition sites, namely for enterokinase, thrombin and factor Xa. After further research on the pET system, an expression vector exhibiting all the features needed was found. It is a pET-45b vector carrying an N-terminal His-tag coding sequence followed by an enterokinase recognition site sequence, which enables a clean-cut with enterokinase proteases. An

Enterokinase Cleavage Capture Kit from Novagen has all the necessary components to treat fusion proteins. The recombinant enterokinase available in this kit recognizes the identical cleavage site (AspAspAspAspLys↓) such as the native enzyme and has similar enzymatic activity, however with superior rates of cleavage. According to Novagen, the enterokinase is purified near homogeneity and exhibits no secondary cleavage.

3.3 pET-45b Expression Vector

Apart from a His-tag coding sequence, as previously described, the pET-45b expression vector also contains a coding sequence for the use of an S-tag if preferred. The replicon, which controls the copy number of the plasmid (del Solar and Espinosa, 2000) is of pBR322 origin (ori) and allows for 15-60 copies/cell (copy number).

The promoter, which controls the transcription of the target protein, is a T7 promoter. The use of T7 can in successful cases express target protein up to 50% of the total cell (Baneyx, 1999; Graumann and Premstaller, 2006). The T7 promoter is recognized by the highly active T7 RNA polymerase (T7 RNAP). The encoding gene of the T7 RNAP is usually inserted in the bacterial genome in a lysogen of λDE3, such as BL21(DE3), under control of the *lacUV5* promoter (Novagen). This type of system can be induced by lactose or its analogue isopropyl-β-D-1-thiogalactopyranoside (IPTG).

The selection marker is a gene encoding resistance for ampicillin and introduced to the plasmid backbone to confer artificial selection and prevent growth of plasmid-free cells. The gene coding for ampicillin resistance is the *bla* gene, encoding the β-lactamase, which is a periplasmic enzyme that inactivates the β-lactam ring in ampicillin. A disadvantage of β-lactamase is that it is continuously secreted and continuously degrading ampicillin (Korpimaki *et al.*, 2003). Eventually, this means that ampicillin will be depleted in a couple of hours and result in growth of plasmid-free cells. *Table 3.1* summarizes the features present in this expression vector.

Table 3.1. Features present in the pET-45b vector.

Replicon	pBR322 origin
Promoter	T7 promoter
Selection Marker	Ampicillin resistance
Affinity Tag	His-tag coding sequence, S-tag coding sequence

Chapter 4

Approaches For Production of Recombinant Human S100 Proteins

This chapter focuses on the approaches used in this project to express recombinant S100 proteins. The project has two distinct approaches in producing recombinant human S100A8 – one, which is expressed fused to a His_6-tag (His_6-rhS100A8) and the other, which is expressed in its wild-type form (wt-rhS100A8). An ambition was also to form heterocomplexes of wt-rhS100A8 and wt-rhS100A9.

4.1 Soluble and Insoluble Proteins

Prior to the large-scale production of the recombinant human S100A8, a small-scale production was performed to i) test the expression and ii) study the nature and yield of the proteins in its soluble and insoluble form, existing as inclusion bodies.

In heterologous expressions, approximately 70-80% of recombinant proteins expressed in *E. coli* exist in inclusion bodies (Yang et al., 2011). The other 20-30% are proteins in their native form and soluble in the cytoplasm, hence they are referred as soluble proteins. The inclusion bodies, in contrast, are insoluble in the cytoplasm. They are highly aggregated, inactive proteins that are a result of high-level expression of many recombinant proteins in *E. coli.* This is very common in heterologous expressions (Fahnert *et al*., 2004), for example expressing human genes in bacteria, which is the case of this project. In one hand, the insoluble proteins are highly expressed, but on the other hand they require time-consuming denaturing and refolding processes in order to become solubilized and obtain their native form, hence also their functionality. The soluble proteins are not as highly expressed but they are already functional in their native form. The decision to continue working with soluble or insoluble proteins is much dictated by the nature of the protein, for example protein stability. It could also be dependent on the quality of the denaturing/refolding processes, if they are good enough to generate sufficient amounts of functional proteins.

4.2 Production of Recombinant wt-hS100A8

The first approach to produce human S100A8 was to express it as recombinant wild-type human S100A8. The used expression vector was a pF1A T7 Flexi® Vector which allows for 15-20 copies/cell. This vector contains a wt-hS100A8 cDNA inserted in the *Sgf* and *Pme*I site of the vector and a β-lactamase gene. *Table 4.1* summarizes the features present in this vector.

Table 4.1. Features present in the pF1A T7 Flexi vector.

Replicon	ColE1-derived
Promoter	T7 promoter
Selection Marker	Ampicillin resistance
Affinity Tag	None

The vector was transformed into *E. coli* BL21(DE3). To verify the expression of proteins, a small-scale cultivation was performed. The small-scale cultivation was used as a guideline as how the large-scale production should be performed to obtain soluble and insoluble proteins. Samples were taken at different hours after induction and analyzed on SDS-PAGE and Western blot. Once the expressed proteins from the small-scale production could be detected and identified with Western blot, a large-scale cultivation was performed subject to the same conditions and parameters as the small-scale cultivation.

4.3 Production of Recombinant His_6-hS100A8

The second approach was to express hS100A8 as a recombinant protein fused to a His_6-tag. The vector of choice was the pET-45b vector, as previously described. This vector contains a human S100A8 cDNA cloned and inserted in the *Kpn*I and *Pac*I sites of the vector. *Figure 4.1* shows a schematic overview of the key elements in the expression vector. Each box represents the DNA sequences, which codes for the His_6-tag, the recombinant enterokinase (rEK) recognition site and human S100A8 at the protein level. A detailed version of the vector can be found in *Appendix I*. The theoretical molecular weight of the His_6-rhS100A8 is 13 kDa and consists of 112 amino acids.

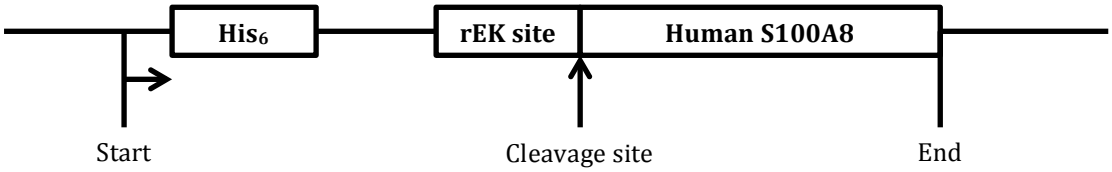

Figure 4.1. Schematic overview of key elements in the expression vector. Each box represents the DNA sequence encoding for the respective amino acid sequence.

This vector was also transformed into *E. coli* BL21(DE3). To verify the expression of proteins, a small-scale cultivation was performed. Similar to the expression of wt-rhS100A8, the small-scale cultivation was used as a guideline as how the large-scale production should be performed to obtain soluble and insoluble proteins.

4.4 Production of Recombinant wt-hS100A8/S100A9

For the production of wt-rhS100A8/S100A9, the wt-rhS100A8 and wt-rhS100A9 were expressed as inclusion bodies (insoluble form) in order to be denatured and refolded into heterodimers. A stock from the cell bank containing transformed BL21(DE3) with pF1A T7 Flexi® Vector was used for the expression of recombinant wt-hS100A8 subject to the same cultivation conditions and parameters as above.

A stock from another cell bank containing successfully transformed BL21(DE3) was used for the expression of recombinant wt-hS100A9. The expression vector was a pET-11/20 vector (a gift) containing a wt-hS100A9 cDNA, inserted in the *Nde*I and *Bam*HI sites of the vector. This vector has a β-lactamase gene but is void of the *lac* repressor gene. *Table 4.2* summarizes the features present in this vector.

Table 4.2. Features present in the pET-11/20 vector.

Replicon	pBR322 origin
Promoter	T7 promoter
Selection Marker	Ampicillin resistance
Affinity Tag	None

Cultivation was directly performed in large-scale as verification of the expression has previously been performed both in-house (for recombinant wt-hS100A9) and from the first approach (for recombinant wt-hS100A8).

Prior to the purification step, the insoluble proteins were denatured and refolded. Refolding is a crucial step to obtain functional proteins out of inclusion bodies. The proteins were first dissolved and denatured with urea and then refolded by dialysis into their natural conformations, which allows for dimerization. Heterodimers of wt-rhS100A8 and wt-rhS100A9 were obtained by mixing equal volumes of both proteins into the dialysis tubes. An approach was also to form homodimers of wt-S100A8 and wt-S100A9, using the latter as a reference to the heterodimers in coming experiments.

Chapter 5

Purification and Characterization Techniques

This chapter describes the techniques used to purify and characterize the S100 proteins. This part contains complementary theoretical information necessary to understand the practical parts of the project.

5.1 Purification of Recombinant wt-hS100A8 and Recombinant wt-rhS100A8/S100A9

Purification of wt-rhS100A8 and wt-rhS100A8/S100A9 were performed using ion-exchange (IEX) chromatography and size-exclusion chromatography (SEC) run on an ÄKTA System.

Briefly, in IEX chromatography, proteins are separated based on reversible interactions between the proteins' net surface charge and the immobilized ion exchange groups (stationary phase) with the opposite charge (GE Healthcare). The net surface charge of a protein is much dependent on the pH of the mobile phase. When the pH of the mobile phase is above the proteins' isoelectric point, (pI) the proteins will bind to a positively charged anion exchanger. With a pI of 6.5 for hS100A8 and 5.7 for hS100A9, using a buffer with a pH of 8.5 both proteins will bind to this strong anion exchanger. The proteins can be eluted with increasing ionic strength using a salt (NaCl) concentration gradient. The increasing salt concentration increases the number of ions competing with the proteins for the charged groups on the stationary phase. The salt ions will ultimately overcome the interaction between the protein and the charged groups, causing the proteins to elute from the column in order of increasing net charges (REACH Devices).

In SEC, proteins are separated based on their size and molecular weight. Using columns packed with porous beads with different pore sizes, the larger proteins, which cannot penetrate the pore system, will elute early together with the void volume (GE Healthcare). This is because they pass the column with the same speed as the flow buffer. In a well-packed column, the void volume is approximately 30% of the total column volume. Proteins with partial access to the pore system will elute in the order of decreasing size. The small proteins, which can penetrate more regions of the pore system will elute last, but cannot

be separated from each other. Normally, they elute just before one total column volume of buffer has passed through the column. The column used in the purification step can separate molecules within discrete separation range intervals from relative molecular weight of 10^2 to 6×10^5 (GE Healthcare).

5.2 Purification of Recombinant His_6-hS100A8

One of the main reasons this project exists is that fusing S100A8 to a tag would facilitate the purification step. Tagging could allow for single-step purification (depending on method), hence numerous chromatography steps can be omitted. His-tagged proteins can be recovered by using immobilized metal ion affinity chromatography (IMAC) with resins loaded with Cu^{2+}, Ni^{2+}, Zn^{2+} or Co^{2+}. *Figure 5.1* shows the affinities and specificities of the metal ions towards histidine. While Co^{2+} has high specificity, the affinity is low. This option is good to reduce non-specific protein binding (Jena Bioscience). Ni^{2+} and Zn^{2+} could be used if specificity and affinity are required.

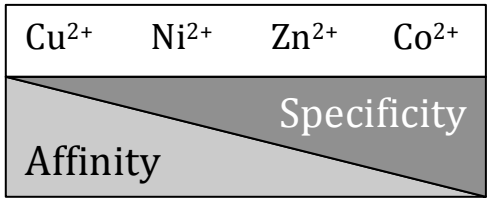

Figure 5.1. Affinity and specificity of metal ions to histidine.

An investigation aimed to find an IMAC column that could enable single-step purification, is compatible with the ÄKTA Systems and also which is compatible with reducing agents. The most suitable column, which has all the required features, is a cOmplete His-Tag Purification Column from Roche. This column consists of a Ni^{2+} chelate matrix and can purify His-tagged proteins both under native and denaturing conditions and rarely interferes with the protein function (Roche). The His-tagged proteins binds specifically to the resin via Ni^{2+}, while most untagged proteins do not. The bound proteins are eluted using an imidazole gradient. The imidazole competes for coordination sites at Ni^{2+} and therefore displaces the His-tagged proteins from the resin, thus causing the proteins to elute from the column.

5.3 Liquid Chromatography–Mass Spectrometry

Liquid chromatography-mass spectrometry (LC-MS) was used to determine the exact masses of the purified protein preparations. LC-MS is an analytical chemistry technique, which combines the physical separation with mass analysis. The physical separation is performed by liquid chromatography and the mass analysis by mass spectrometry.

Briefly, liquid chromatography operates at relatively high pressure using a high-pressure pump and a column with small chromatographic packing materials (stationary phase)(Waters). An injector introduces the sample into a continuous flowing mobile phase. The sample is forced through the column by the mobile phase at high pressures, which is generated by the high-pressure pump. This is referred to as high performance liquid chromatography (HPLC). In this experiment, reversed-phase HPLC (RP-HPLC) was used in combination with MS. In contrast to normal phase chromatography, which uses a hydrophilic stationary phase, RP-HPLC uses organic-modified particles to create a hydrophobic stationary phase (Guzzetta, 2001). The separation is based on the molecules' hydrophobicity – the more hydrophobic the protein (or molecule), the more strongly it binds to the alkyl chains in the stationary phase, which makes the hydrophobic milieu. Alkyl chains are commonly C4, C8 and C18, where C4 is generally used for proteins. When the RP-HPLC separates the sample, the molecules (i.e. proteins and other contaminant molecules) enter the MS in the order in which they are separated, i.e. the least hydrophobic molecules enter the MS first.

MS is an analytical technique that can be used to determine the mass of a molecule. The MS works by ionizing the molecules to gas-phase ions. Ionization methods include laser ablation, electron ionization (IE) and electrospray (ESI) (Waters). The charged molecules (ions) are then separated according to their mass-to-charge ratios (m/z) in an electromagnetic field applied by a mass analyzer. The charged molecules are then measured according to their mass-to-charge ratios in a detector.

5.4 Biacore Surface Plasmon Resonance

Biacore was used to study the *in vitro* interactions between the S100 proteins and different ligands immobilized on a chip. Briefly, Biacore is an analytical instrument based on surface plasmon resonance (SPR) (GE Healthcare). It is a real-time, label-free detection and characterization of bimolecular interactions, particularly between proteins and other molecules.

Biacore uses sensor chips to monitor molecular interactions by an SPR detector (GE Healthcare). Samples and buffers are delivered to the chip by a microfluidic

system. The sensor chip constitutes of a glass slide thinly coated with gold. This surface is normally covered in covalently attached dextran matrix acting as a substrate to which ligands can be covalently coupled, known as immobilization. The analytes (molecules that bind to the ligands), which are present in a solution, is continuously injected over the surface where the ligands are present. SPR uses polarized light to strike the surface of the glass side. As analytes bind to the ligands, it alters the refractive index and hence also the angle of the reflected intensity of light. The changes in angle are proportional to the mass of the analytes. *Figure 5.2* shows the basic instrument configuration.

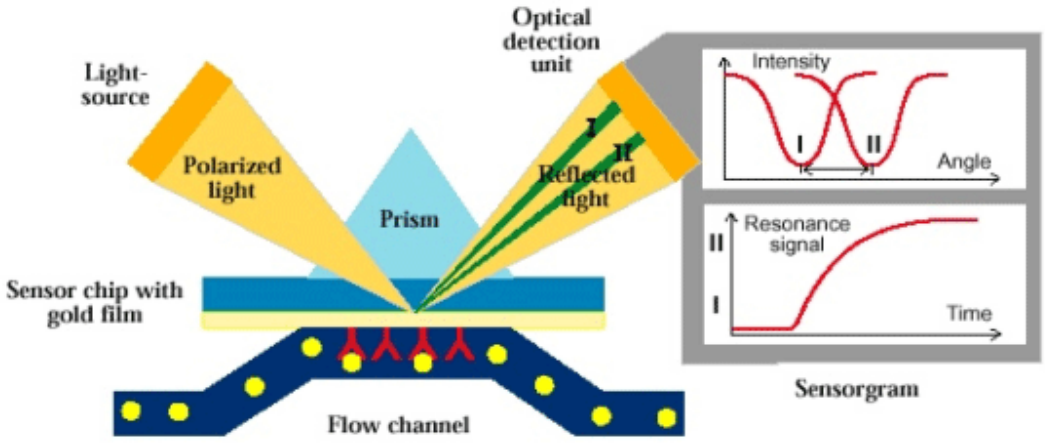

Figure 5.2. Basic SPR instrument configuration (*Biacore, 2003*).

In this experiment, chips immobilized with TLR4-MD2, RAGE and monoclonal antibodies (mAbs) were used (immobilization performed by Active Biotech). The used mAb clones were 8-5C2 and 27E10 from BMA Biomedicals. The mAb 8-5C2 is an anti-S100A8 and detects a very distinct epitope in the central part of the protein in between the two Ca^{2+} binding sites. The mAb 27E10 is an anti-S100A8/S100A9 and detects an epitope, which only occurs on the heterocomplex and not on the individual subunits.

5.5 NF-κB Luciferase Reporter Assay

To characterize the S100 proteins in terms of activating the signalling pathway of NF-κB, a technique called NF-κB Luciferase reporter assay can be used. The assay was used to measure the activities of the recombinant proteins in a cell-based *in vitro* in terms of binding to receptors that activate the NF-κB signalling pathway. A vector containing firefly luciferase genes downstream of NF-κB response elements is used to transfect cells. When NF-κBs, present inside of the cells, are activated through extracellular signals via receptors, the NF-κBs will migrate into the nucleus and bind to the NF-κB response elements. When bound to these response elements, it induces the transcription of the luciferase reporter genes. The expressed luciferase, which is an enzyme, catalyses the oxidation of

small substrates called luciferins. As a result, luciferin converts into an excited electronic state, and when it reverts back to ground state, luminescence is emitted (Chauvin, 2011). This luminescence can be detected by a luminometer and the signals can be measured. The substrate, which contains luciferins, is added to the cells right before it is time to perform the measurements.

In this experiment, HEK293 (Human Embryonic Kidney 293) cells, which are genetically modified to express abundant TLR4-MD2 (Active Biotech AB) and contains an NF-κB Luciferase reporter system, were used to measure the stimuli via the TLR4-MD2 by the S100 proteins.

Chapter 6

Materials and Methods

6.1 Protein Expression

Transformation of BL21(DE3) with expression vectors was performed by heat shock according to Novagen's Competent Cells User Protocol (TB008 Rev. F 0104). Bacteria were plated on agar containing 100 µg/mL ampicillin. Single colonies were inoculated in 2×YT medium with 100 µg/mL ampicillin. When using cell banks of verified transformed cells, stocks were added to 2×YT medium with 100 µg/mL ampicillin. The pre-cultivation proceeded at 25°C, 225 rpm overnight (approximately 18 h). The following day, pre-cultivation was used to inoculate larger volumes of 2×YT medium with 100 µg/mL ampicillin to a final OD_{620} of 0.1. Bacteria were then grown at 37°C. When OD_{620} reached 0.7-1 the bacteria were induced with isopropyl β-thiogalactoside (IPTG) to a final concentration of 0.5 mM and subsequently grown at 37°C for 3 hours to obtain soluble proteins and over night (approximately 21 hours) to obtain insoluble proteins (inclusion bodies). After incubation, the bacteria were centrifuged (8000 × g, 30 min, 5 °C) and the supernatant was discarded. Small-scale cultivation was performed with 2×25 mL medium and large-scale cultivation was performed with 5×400 mL medium.

6.2 Protein Extraction and Protein Preparation

Extraction of soluble and insoluble proteins in small-scale was performed according to Novagen's protocol for BugBuster® Protein Extraction Reagent (TB245 Rev. D 0903). Protein extraction in large-scale was performed with freeze-thawing in 25 mM Tris, 1 mM EDTA, pH 8.5 together with 25 U/µL Benzoase (Novagen) and cOmplete Mini Protease Inhibitors (Roche), followed by sonication (15 sec sonication + 15 sec pause, 3 times). The lysate was then centrifugation (30 min, 20 000 × g, 4°C) and the supernatant was collected. The supernatant was filtered over combined GF/0.45 µm Minisart (Satorious). To avoid possible disulfide bonds between the proteins dithiothreitol (DTT), a reducing agent, was added in all stages following protein extraction.

6.3 Resuspension, Denaturing and Refolding

Inclusion bodies were resuspended in 8 M Urea, 40 mM DTT in 500 mM NaH_2PO_4, pH 1.8. When homogeneous, the solution was centrifuged (20000 × g, 5°C, 30 min) and the supernatant containing the solubilized proteins from inclusion bodies was filtered over combined Minisart-GF prefilter and 0.45 µm Minisart filter (Sartorius Stedim Biotech).

Refolding was performed in five dialysis steps, all performed in Spectra/Por® 3 Dialysis tubes (Spectrum Laboratories Inc.), MWCO 3500 (Molecular Weight Cut-Off). First dialysis was against 50 mM NaH_2PO_4 buffer, 10 mM DTT, pH 2 for 6 h. Second dialysis was against 10 mM Na-acetate buffer, 150 mM NaCl, 10 mM DTT, pH 4 for 16 h. Third dialysis was against 10 mM Na-acetate buffer, 150 mM NaCl, 10 mM DTT, pH 4 for 8 h. Fourth dialysis was against 20 mM Tris-HCl, 150 mM NaCl, 10 mM DTT, pH 7. For 16 h. Fifth dialysis was against 20 mM Tris-HCl, 1 mM EDTA, 1 mM EGTA, 10 mM DTT, pH 8.5 for 6 h. The final solution was centrifuged (25000 × g, 5°C, 30 min). The supernatant was then filtered over 0.45 µm Minisart filter (Sartorius Stedim Biotech) prior to the first purification step.

Refolding of wt-rhS100A8 and wt-rhS100A9 was also performed as a method of forming heterodimer complexes. Complex formation was enabled by mixing equivalent volumes of each protein in a dialysis tube.

6.4 Purification by Chromatography

All chromatography steps were run on an ÄKTAexplorer 100 (GE Healthcare). The wavelength detection is at 280 nm. Recombinant wt-hS100A8 and recombinant wt-hS100A9 proteins were purified using anion exchange chromatography and size-exclusion chromatography.

The first purification step was with anion-exchange chromatography on a HiPrep Q FF 16/10 column (GE Healthcare). A buffer with 20 mM Tris, 1 mM EDTA, 1 mM EGTA, 10 mM DTT, pH 8.5 was used for equilibration and washing before elution. A 0-1 M NaCl gradient in the same buffer was used for elution of proteins. Proteins can be tracked on a chromatogram and traced to the fractions containing the proteins. Samples containing proteins were then analyzed on SDS-PAGE to study the homogeneity. If there were still a lot of contaminants, the fractions containing the proteins were pooled and run on a second anion-exchange chromatography column.

The second purification step was with anion-exchange chromatography on a SOURCE 15Q 4.6/100 PE column (GE Healthcare). The SOURCE 15Q has a higher polishing effect, higher resolution and higher throughput (GE Healthcare) than the HiPrep Q FF 16/10 column. The SOURCE 15Q column was run using the same buffer and gradient for equilibration, washing and elution. Again, if the SDS-PAGE gel shows that there were still a lot of contaminants, the fractions containing the proteins were pooled and run, only this time, on a size-exclusion chromatography column.

The third purification step was with size-exclusion chromatography on a Superdex 75 11/790 column (GE Healthcare). The column was run using a HBS-N buffer (0.01 M Hepes pH 7.4, 0.15 M NaCl, GE Healthcare) supplemented with 10 mM DTT. This column can separate molecules within discrete separation range intervals from relative molecular weight of 10^2 to 6×10^5 (GE Healthcare).

Recombinant His_6-tagged hS100A8 proteins were purified using immobilized metal ion affinity chromatography on a nickel cOmplete His-Tag Purification column (Roche). A buffer with 50 mM NaH_2PO_4, 300 mM NaCl, pH 8.0 was used for equilibration and washing before elution. A 0-250 nM imidazole gradient in the same buffer was used for elution of proteins.

All column was then washed and stored in 20% Ethanol.

6.5 Cleavage of Recombinant His_6-hS100A8

A small-scale optimization was performed for cleavage of the recombinant His_6-tagged rhS100A8 proteins from its tag. Recombinant Enterokinase (rEK) purchased from Novagen was used for digestion of the protein in accordance with Novagen's User Protocol for Recombinant Enterokinase (TB150 Rev. C 0107). The experiment was designed to estimate the appropriate enzyme:target ratio. Several rEK concentrations, temperatures, buffers and incubation times were tested to optimize the cleavage. Starting off, samples were tested with an approach provided as an example by Novagen.

The first approach used a constant amount of protease (1 U) added to three different amounts of target protein; 20, 50 and 74 µg. The samples were then analyzed at increasing incubation time in room temperature. Samples were taken after 2, 4, 6, 7, and 16 hours and analyzed with SDS-PAGE.

The second approach did not use a constant amount of protease but instead 1, 5 and 10 U was added to 20 and 50 µg of target proteins. Another modification was that DTT was added to the protein solution to a final concentration of 10 mM. The third modification was that doublets of the samples were prepared so that the exact same composition could be tested both in room temperature and in 4 °C. A fourth modification was that the reactions were incubated over the weekend. Samples were taken after the weekend and analyzed with SDS-PAGE.

The third approach used, instead of the rEK Cleavage/Capture Buffer provided in the kit, a new buffer that is almost identical but lacks $CaCl_2$. Incubation time was 16 hours in room temperature and samples were taken for SDS-PAGE analysis.

6.6 Buffer Exchange and Endotoxin Removal

Fractions containing proteins were pooled and concentrated in a Centriprep Ultracel® YM-3 centrifugal filter, 3000 NMWL (Nominal Molecular Weight Limit) (Millipore) before loading on a PD-10 Desalting Column (GE Healthcare) for buffer exchange to HSB-N buffer (10 mM HEPES, 150 mM NaCl, pH 7.4, GE Healthcare, Sweden), according to GE Healthcare's instructions (52-1308-00 BB). Fractions from the buffer exchange containing proteins were yet again pooled and concentrated in a Centriprep Ultracel® YM-3 centrifugal filter, 3000 NMWL (Millipore) before loading on a Detoxi-Gel™ Endotoxin Removing Column (Thermo Scientific), performed according to their instructions (0415.5).

6.7 Protein Concentration Determination

The protein concentration was determined by UV adsorption at 280 nm with a diode array detector HP8453-UV spectrophotometer (Hewlett-Packard, Germany) using a molar extinction coefficient of 0.83 M^{-1} cm^{-1} for His_6-S100A8, 0.62 M^{-1} cm^{-1} for S100A9, and 0.75 M^{-1} cm^{-1} for S100A8/S100A9 heterocomplex. The molar extinction coefficients are based on the amino acid composition.

6.8 Limulus Amebocyte Lysate Assay (LAL)

A Limulus Amebocyte Lysate Assay (LAL assay) was used to quantify and detect gram-negative bacterial endotoxins. The Pierce® LAL Chromogenic Endotoxin Quantification Kit purchased from Thermo Scientific was used and performed according to their instructions (2445.3).

6.9 Liquid Chromatography-Mass Spectrometry (LC-MS)

LC-MS was used to determine the exact masses of the proteins, using an Accela™ Autosampler LC-system (Thermo Scientific) and an LTQ XL™ MS-system (Thermo Scientific). The samples were diluted to 100 µg/mL with dH_2O and DTT was added to a final concentration of 2 mM. An xBridge™ BEH C_4, 300Å, 3.5 µm 21×150 mm column (Waters) and mobile phases acetonitrile + 0.1% TFA (trifluoroacetic acid) and dH_2O + 0.1% TFA were used for LC-MS analysis. Protocol by Mats Nilsson (Active Biotech).

6.10 Biacore SPR

Biacore Surface Plasmon Resonance (SPR) was used to test *in vitro* bindings of the proteins to mAb, recombinant human RAGE and recombinant human TLR4-MD2, using a Biacore® 3000 (Biacore-GE Healthcare) and CM5 research grade sensor chips (Biacore-GE Healthcare) with immobilized ligands/antibodies prepared by Active Biotech. Receptor ligands rhRAGE and rhTRL4 were purchased from R&D Systems. The mAbs clone 8-5C2 (anti-hS100A8) and clone 27E10 (anti-hS100A8/S100A9) were purchased from BMA Biomedicals. Protein samples were diluted to 100, 50, 25, 12.5, 6.25 and 3.125 nM when testing for antibody binding. Proteins were diluted to 400, 200, 100, 50 and 25 nM when testing for receptor binding. The buffer of use for dilutions was HBS-P buffer

(0.01 M HEPES pH 7.4, 0.15 M NaCl, 0.005% v/v Surfactant P20, GE Healthcare) with 5 mM Ca^{2+} and 150 μM Zn^{2+}.

6.11 Nf-κB Luciferase Assay

HEK293 cells (human embryonic kidney cell line) genetically modified to express abundant human TLR4-MD2 (Active Biotech) and containing an NF-κB Luciferase reporter system, were continuously cultivated in T_{75} flasks in 37 °C, 5% CO_2, 90% relative humidity in cultivation medium containing RPMI medium (LONZA), 10% fetal bovine serum (FBS). One day ahead of the assay experiment, cells in a T_{75} flask were washed with phosphate-buffered saline (PBS) and detached from the flask with trypsin. Cells were then resuspended with RPMI medium without phenol red (LONZA) supplemented with 1% FBS and 0.2 mM L-glutamine, followed by centrifugation (1200 rpm, 5 min). After counting of cells, they were resuspended in the same medium as above to a final concentration of 5×10^5 cells/mL. The cell suspension was added to a 96-well optiplate (100 μL/well) and incubated in the same condition as above over-night. At the day of the experiment, 50 μL was aspirated from each well, and then 50 μL of RPMI medium without red phenol and 20 μM $ZnCl_2$ containing the proteins were added to final protein concentrations of 0.4 and 0.15 μM. Blanks and controls of a final concentration of 50 pg LPS/mL were also added to the wells. The cells were then incubated in the same conditions as above for 4 hours. After incubation, the plate was left for 15-20 minutes to cool to room temperature before adding 100 μL of lyophilized steadylite plus™ substrate solution (PerkinElmer). The plate was then put on a shaker for 15 minutes before measuring the NF-κB activity as luminescence in a luminometer (LUMIstar Galaxy). Protocol by Anneli Nilsson (Active Biotech).

6.12 SDS-PAGE Analysis

SDS-PAGE was used to estimate the molecular weight of the proteins. The protein samples were separated on the same gel as a molecular weight standard. The SDS-PAGE gel, a 4-12% 1.5 mm Bis-Tris gel (Invitrogen) were run according to the manufacturer's instructions with NuPAGE MES SDS Running Buffer (Invitrogen), plus 10 mM DTT in upper chamber. Protein samples were mixed with NuPAGE LDS Sample Buffer (Invitrogen) and NuPAGE Sample Reducing Agent (Invitrogen). Precision Plus Protein™ Dual Color Standards (Bio-Rad Laboratories) were used as the molecular weight standard. Gels were run on POWER PAC 300 (Bio-Rad) at 200 V for 35 minutes and then washed in dH2O before staining with SimplyBlue™ SafeStain (Invitrogen) according to instructions.

6.13 Western Blot Analysis

Western blot was used to detect and identify the proteins. The protein samples were firstly separated on SDS-PAGE gels (Bis-Tris gels) and transferred to PVDF Membrane Filter Paper Sandwich, 0.2 μm Pore Size (Invitrogen, USA) run on an

Electrophoresis Power Supply EPS 200 (Pharmacia Biotec) in 100 V, 400 mA for 1 hour with transfer buffer (25 mM Tris, 192 mM Glycine, 20% (v/v) Ethanol). Membranes were blocked in Tris-buffered Saline and Tween 20 (TBST), 5 % milk powder for 1 hour followed by probing with primary antibodies overnight at 4°C. Goat polyclonal IgG Calgranulin A (0.2 mg/mL, sc-8112, Santa Cruz Biotechnology Inc.) was used as primary Ab against S100A8 in the dilution range 1:1000 in TBST, 5% milk powder. Goat polyclonal IgG Calgranulin B (0.2 mg/mL, sc-8114, Santa Cruz Biotechnology Inc.) was used as primary Ab against S100A9 in the dilution range 1:1000 in TBST, 5% milk powder. The following day, membrane was washed 3 times with TBST (15/5/5 min). The membrane was then incubated with second antibodies (Rabbit anti-goat 1:5000 (DAKO P0160) in TBST, 5% milk powder) for 1-1.5 hours for detection of the primary antibodies. The membrane was washed in TBST 4×10 min before development with Amersham™ ECL™ Western Blotting Reagent (GE Healthcare), Amersham™ ECL™ Prime Western Blotting Detection Reagent (GE Healthcare) or SuperSignal® West Femto Chemiluminiscent Substrate (Thermo Scientific) until detectable by ChemiDoc™ MP Imaging System (Bio-Rad).

6.14 Reference Proteins

Reference proteins used in the experiments are recombinant human S100A8 expressed in *E. coli* and human S100A8/S100A9 purified from granulocytes.

Chapter 7

Results

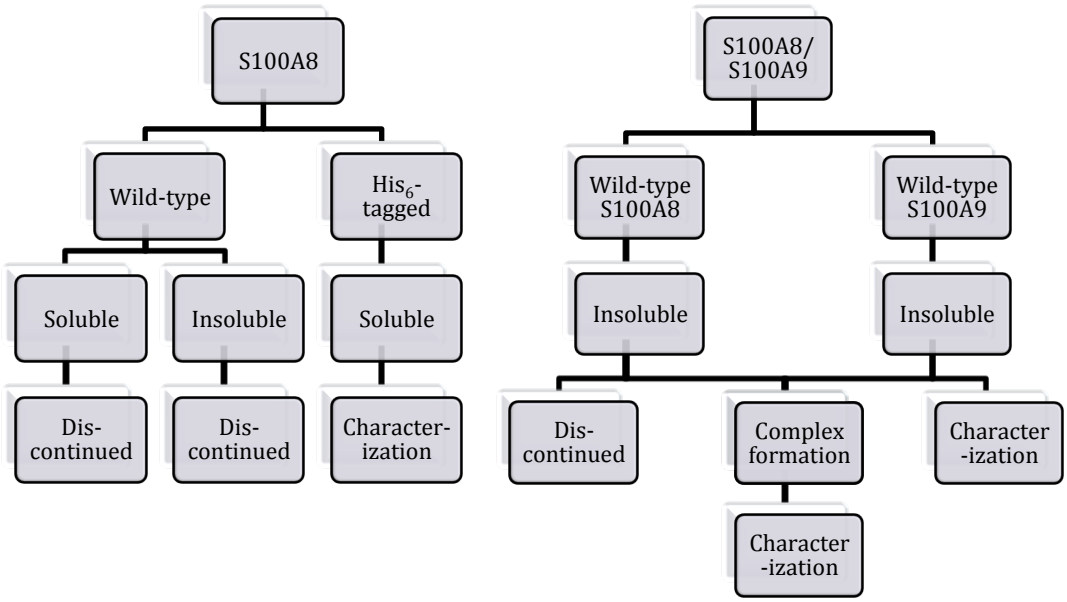

Figure 7.1. Overview of the route to produce recombinant human S100A8 and recombinant human S100A8/S100A9 for characterization.

This chapter includes the most important data over His_6-rhS100A8 and wt-rhS100A8/S100A9 from cultivation to characterization. Data over wt-rhS100A9 was used as reference to the wt-rhS100A8/S100A9 heterocomplex. An overview of the route to produce these recombinant proteins can be viewed in *Figure 7.1*.

7.1 Production of Recombinant wt-hS100A8

7.1.1 Expression of Recombinant wt-hS100A8

In the first approach to produce recombinant human S100A8, the protein was expressed in its wild type form. A small-scale cultivation was performed to study the expression. Samples were taken 0, 2, 3 and 21.5 h after induction to determine the optical density (OD) at 620 nm and to prepare the samples. Preparation of the samples was performed in order to obtain soluble proteins from the soluble fraction and solubilized proteins from the insoluble fraction in the cell. The proteins were then analysed with SDS-PAGE and Western blot. In the SDS-PAGE analysis (*Figure 7.2A*) there are bands present right above the 10 kDa molecular weight marker (MWM) band. A reference rhS100A8 was also loaded on the gel showing bands right above the 10 kDa MWM. With a theoretical molecular weight of 10.8 kDa, the bands might very well represent human S100A8. A Western blot analysis (*Figure 7.2B*) using mAbs specifically against human S100A8, confirmed that the bands were indeed hS100A8. Moreover, the sample containing soluble proteins taken 3 hours after induction shows a faint band (shadow) below the clear band. Since the antibodies could develop the band, it seems to be related to hS100A8. These might correspond to fragmentations of the soluble protein.

From the SDS-PAGE analysis, it can be seen that the expression of soluble proteins increases from 0-3 hours but over night (after 21.5 h), the amount is reduced. The highest amount of soluble proteins was found 2-3 hours after induction. In contrast, the proteins from the insoluble fraction also increase over time but have the highest amount after 21.5 h.

The large-scale cultivation was progressed for 3 hours to obtain proteins in the soluble fraction and 21.5 hours to obtain proteins in the insoluble fraction. The growth curves of small-scale and large-scale cultivation after induction can be viewed in *Figure 7.3*. The OD_{620} for both small-scale and large-scale cultivation at 3 and 21 hours after induction were approximately 4.5-5.

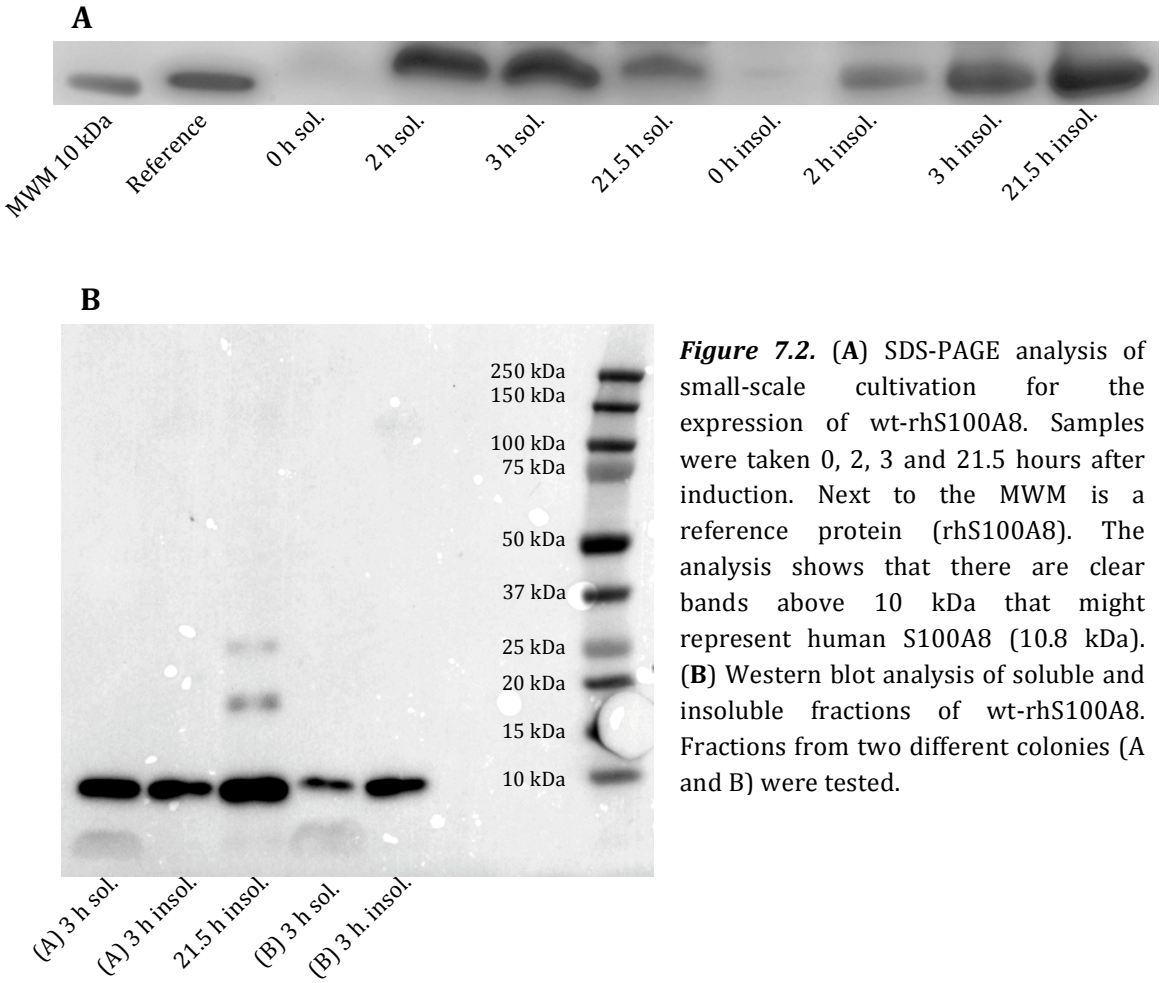

Figure 7.2. (**A**) SDS-PAGE analysis of small-scale cultivation for the expression of wt-rhS100A8. Samples were taken 0, 2, 3 and 21.5 hours after induction. Next to the MWM is a reference protein (rhS100A8). The analysis shows that there are clear bands above 10 kDa that might represent human S100A8 (10.8 kDa). (**B**) Western blot analysis of soluble and insoluble fractions of wt-rhS100A8. Fractions from two different colonies (A and B) were tested.

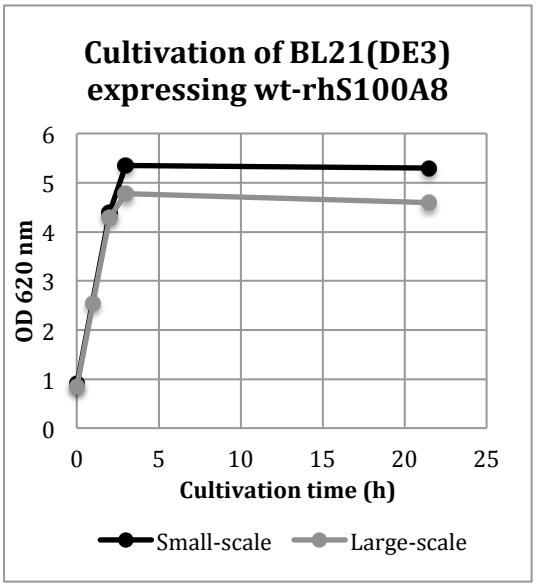

Figure 7.3. Growth curves for cultivation of BL21(DE3) after induction, expressing wt-rhS100A8. OD at 620 nm was measured for both small-scale and large-scale cultivation after 0, 2, 3 and 21.5 hours after induction.

7.1.2 Purification of Recombinant wt-hS100A8

The proteins in the soluble fraction from the large-scale cultivation were extracted and purified by anion-exchange chromatography on a HiPrep Q FF 16/10 column. Samples were collected from fractions at areas showing high absorbance (*Figure 7.4*) and analysed on a SDS-PAGE gel (*Figure 7.5*). The most homogenized fractions (Fr.) that show visible bands just above 10 kDa (Fr. 45-56) were pooled for further purification.

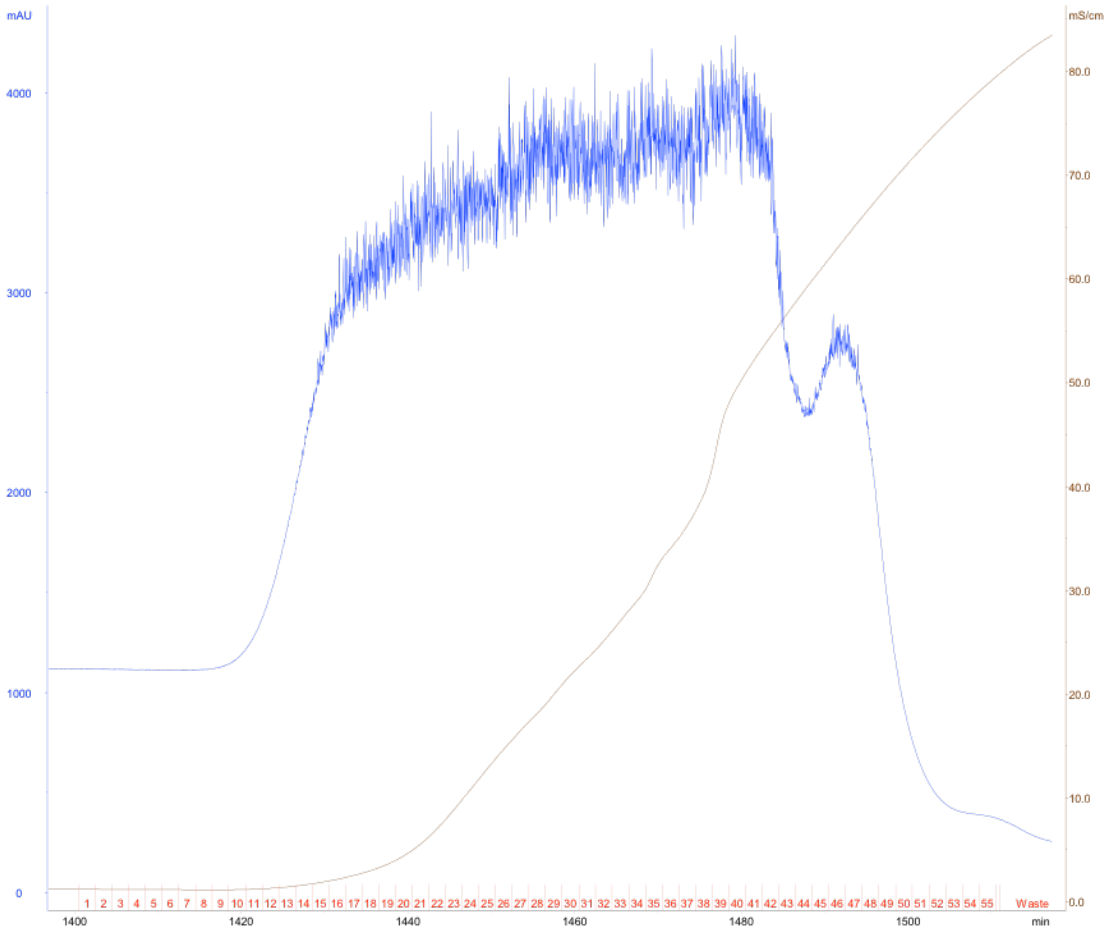

Figure 7.4. Chromatogram of soluble wt-rhS100A8 purified on a HiPrep Q FF 16/10 anion exchange column. The blue Y-axis and graph shows the UV absorbance at 280 nm (mAU) and the brown Y-axis and graph shows conductivity (mS/cm). The X-axis shows time in minutes and the numbers in red are the fraction numbers.

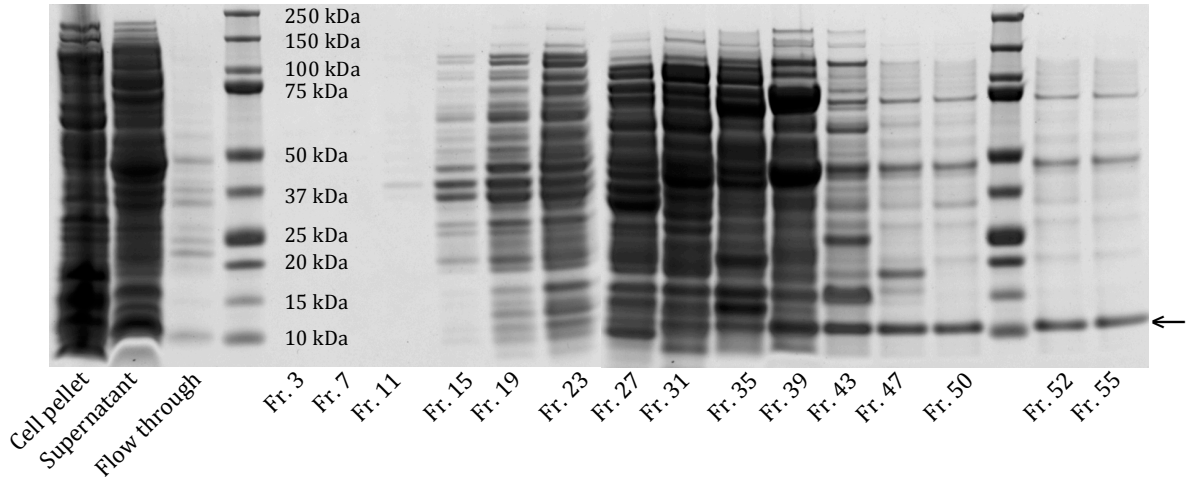

Figure 7.5. SDS-PAGE analysis of fractions containing soluble wt-rhS100A8 after purification on HiPrep Q FF 16/10 anion exchange column. Samples of the flow through (FT), the cell pellet (resuspended) and supernatant from the extraction step were also run on the gel.

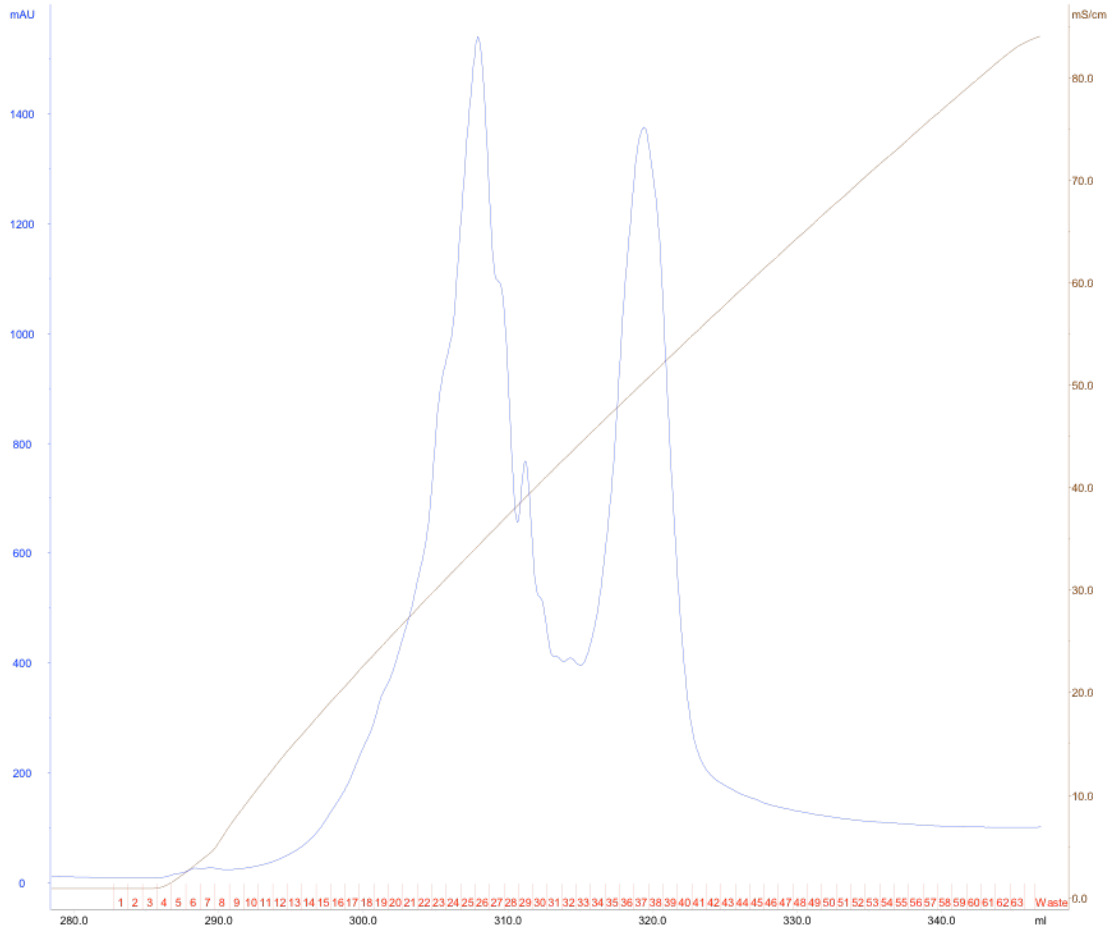

Figure 7.6. Chromatogram from purification of soluble wt-rhS100A8 purified on a SOURCE 15Q 4.6/100 PE anion exchange column. The blue Y-axis and graph shows the UV absorbance at 280 nm (mAU) and the brown Y-axis and graph shows conductivity (mS/cm). The X-axis shows time in minutes and the numbers in red are the fraction numbers.

In the second purification step, the pooled fractions from the first purification step were purified by anion-exchange chromatography on a SOURCE 15Q 4.6/100 PE column. Again, samples were collected from fractions at areas showing high absorbance (*Figure 7.6*) and analysed on a SDS-PAGE gel (*Figure 7.7*). The SDS-PAGE showed weak bands that correspond 10.8 kDa in fraction 24-30. The protein loss could be due to fragmentation as a result of instability, choice of purification or the number of purification steps. Due to lack of material, the production of this batch was discontinued.

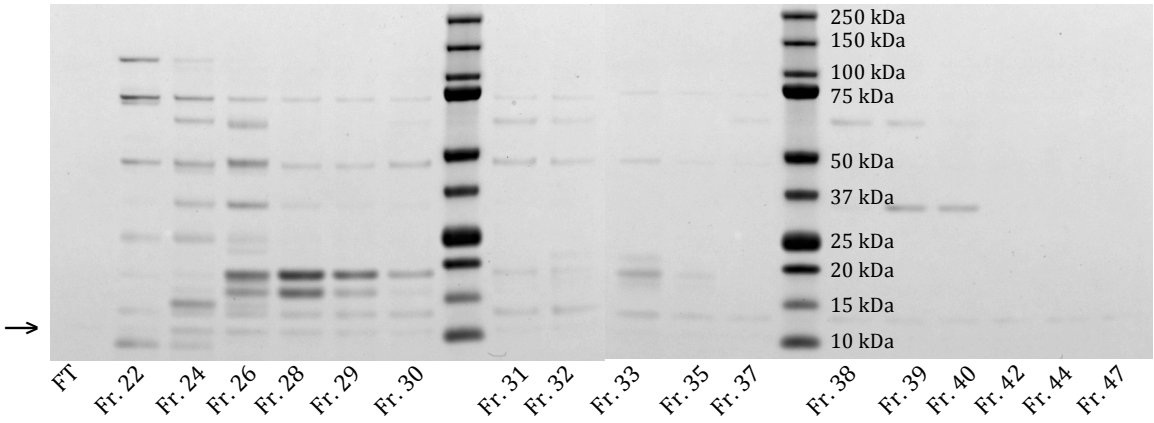

Figure 7.7. SDS-PAGE analysis of fractions containing soluble wt-rhS100A8 from purification with SOURCE 15Q 4.6/100 PE anion exchange column. Sample of the flow through (FT) was also run on the gel.

After extraction, the insoluble proteins from the large-scale cultivation were subject to denaturing and refolding processes to become soluble and functional proteins. They were then purified using the same purification steps and strategies as above. An additional purification step was added using size-exclusion chromatography on a Superdex 75 11/790 column. Samples were collected from fractions at areas showing high absorbance (data not shown) and analysed on a SDS-PAGE gel (data not shown). The fractions showed no bands on the gel. A Western blot analysis could verify that there were proteins before purification on the Superdex 75 11/790 column, but not in the fractions (*Appendix II*). Again, this could be due to fragmentation, choice of purification or protein loss as a result of numbers of purification steps. Due to lack of material, the production of this batch was discontinued. Despite the difficulties to purify wt-rhS100A8 as a homocomplex, the expression of the protein could still be verified by Western blot (*Figure 7.2B*).

7.2 Production of Recombinant wt-hS100A8 and wt-hS100A9 for Preparation of Recombinant wt-hS100A8/S100A9

The strategy to produce heterocomplex of S100A8 and S100A9 started with separate large-scale cultivations for expression of wt-rhS100A8 and wt-rhS100A9 as insoluble proteins. During the cultivations, samples were taken 0, 2.5, 3.5, 4.5 and 21 h after induction to measure the optical density (OD) at 620 nm. The OD_{620} for both cultivations at 21 hours after induction were approximately 4 (*Figure 7.8*).

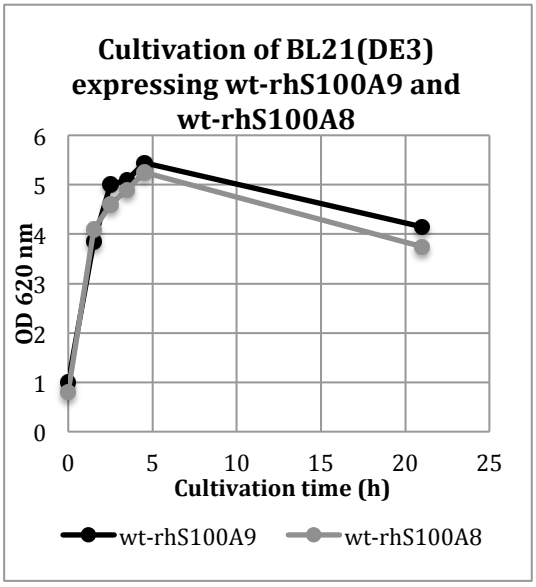

Figure 7.8. Growth curves for cultivation of BL21(DE3) expressing wt-rhS100A8 and wt-rhS100A9. OD at 620 nm was measured after 0, 2.5, 3.5, 4.5 and 21 hours after induction.

After extraction, the proteins were subject to denaturing and refolding processes to become soluble and functional proteins. For preparation of the heterocomplexes, equal volumes of both proteins were added to the dialysis tubes for refolding. The wt-rhS100A8/S100A9 was purified in one step (data not shown) by anion-exchange chromatography on a HiPrep Q FF 16/10 column. The fraction with the strongest bands with equal amounts of wt-S100A8 and wt-S100A9 were collected for further experiments (*Appendix III*). The figure is shown in *Figure 7.9A* cropped as no other bands were visible. As judged by the gel, the purity is >95%. A Western blot analysis was also performed to confirm the identities of wt-rhS100A8 and wt-rhS100A9 in the heterocomplex (*Figure 7.9B* and 7.*9C*).

Portions of the batches containing extracted wt-rhS100A8 and wt-rhS100A9 were used to prepare homocomplexes (second attempt to produce wt-rhS100A8 from insoluble proteins) as reference proteins to wt-rhS100A8/S100A9. The wt-rhS100A9 were purified to homogeneity by anion-exchange chromatography on a HiPrep Q FF 16/10 column (data not shown). The purity of wt-rhS100A9 was analysed with SDS-PAGE (*Figure 7.9D)*. The purification of wt-rhS100A8 proved yet again to be challenging, resulting in protein loss. Hence the production of this batch was discontinued.

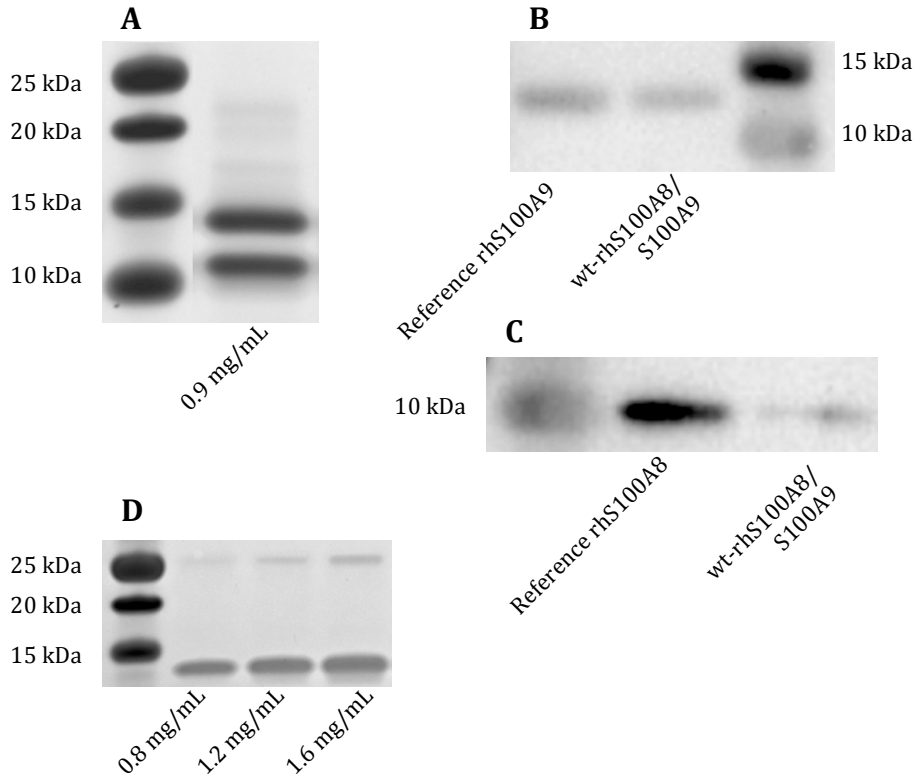

Figure 7.9. (**A**) Purity of wt-rhS100A8/S100A9 heterocomplex (10.8 kDa and 13.1 kDa) analysed with SDS-PAGE. The figure is cropped as no other bands were visible. As judged by the gel, the purity is >95%. (**B**) Identification of wt-rhS100A9 in the heterodimer complex with Western blot. Reference used is a rhS100A9 (**C**) Identification of wt-rhS100A8 in the heterodimer complex with Western blot. Reference used is a rhS100A8. (**D**) Purity of wt-rhS100A9 (13.1 kDa) analysed with SDS-PAGE.

7.3 Production of Recombinant His_6-hS100A8

7.3.1 Expression of Recombinant His_6-hS100A8

In the second approach to produce recombinant human S100A8, the protein was expressed fused to a His_6-tag. A small-scale cultivation was performed to study the expression. Samples were taken 0, 2, 3 and 21.5 h after induction to determine the optical density (OD) at 620 nm and to prepare the samples. Preparation of the samples was performed in order to obtain soluble (cytoplasmic) proteins from the soluble fraction and solubilized proteins from the insoluble fraction. The proteins were then analysed with SDS-PAGE and Western blot. In the SDS-PAGE analysis (*Figure 7.10A*) there were bands present right below the 15 kDa molecular weight marker. With a theoretical molecular weight of 13 kDa, the bands might very well represent His_6-rhS100A8. The SDS-PAGE gel shows strong bands in the soluble fraction 2-3 hours after induction and in the insoluble fraction after 21 hours, the same behaviour as could be seen for the expression of wt-rhS100A8. However, it can also be observed that the molecular weight of the proteins in the soluble and insoluble fractions are different, with the latter having lower molecular weight. This could be due to structural differences between the two, e.g. an deducted amino acid or structural modifications such as oxidation.

A Western blot analysis (*Figure 7.10B*) using mAbs specifically against human S100A8, confirmed that the bands of the soluble fractions were hS100A8 (the insoluble fraction was not analysed). The large-scale cultivation was progressed for 3 hours to obtain high yields of His_6-rhS100A8 in the soluble fraction. *Figure 7.11A* and *7.11B* shows a comparison of cultivations expressing His_6-rhS100A8 versus wt-rhS100A8 in small- and large-scale. In both small- and large-scale, the OD_{620} at 3 hours after induction were higher for the cultivation of wt-rhS100A8, but at 21 hours after induction they both reach the same OD_{620} of approximately 5.

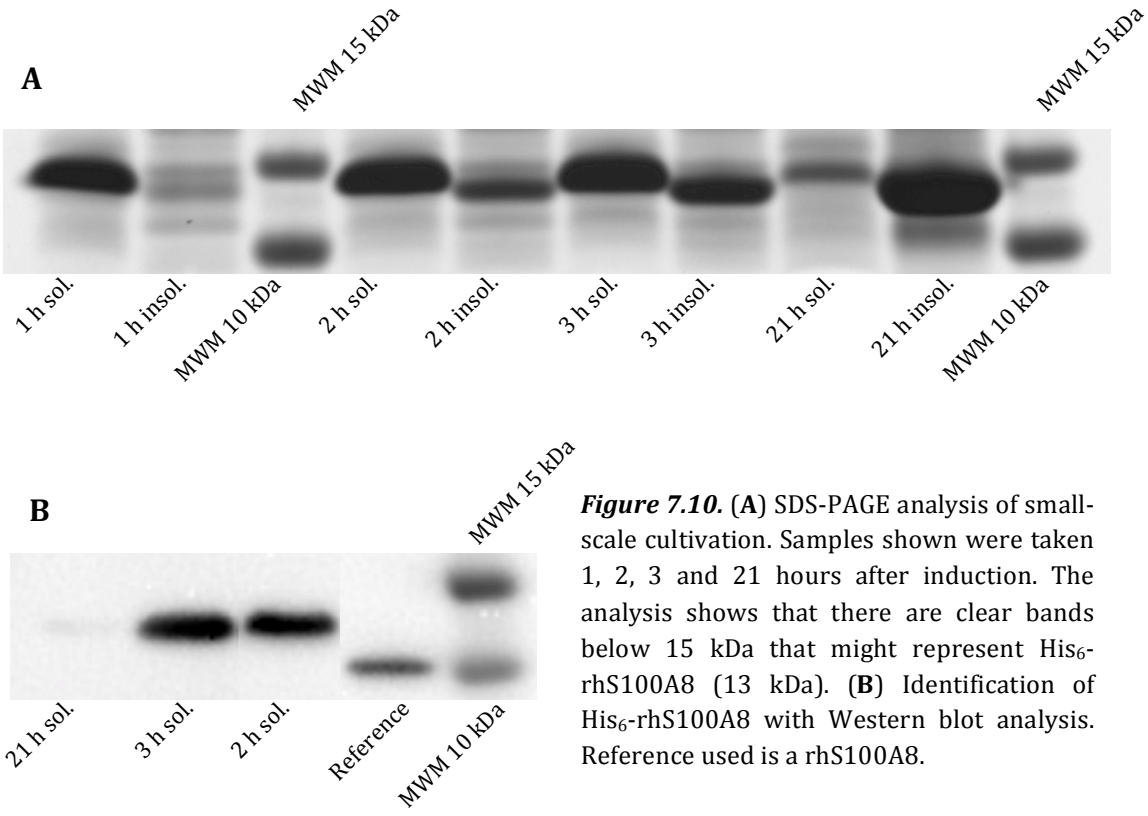

Figure 7.10. (**A**) SDS-PAGE analysis of small-scale cultivation. Samples shown were taken 1, 2, 3 and 21 hours after induction. The analysis shows that there are clear bands below 15 kDa that might represent His_6-rhS100A8 (13 kDa). (**B**) Identification of His_6-rhS100A8 with Western blot analysis. Reference used is a rhS100A8.

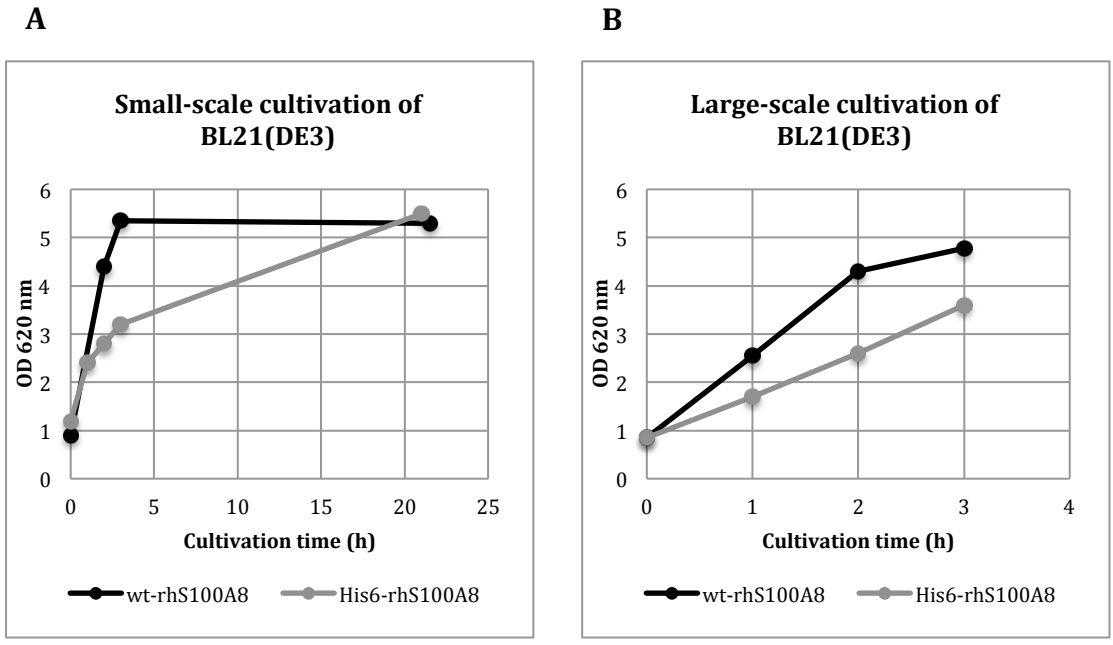

Figure 7.11. Growth curves of cultivation for BL21(DE3) expressing His_6-rhS100A8 versus wt-rhS100A8. OD at 620 nm was measured for both small-scale and large-scale cultivation 0, 1, 2, 3 and 21 hours after induction. (**A**) Comparison of small-scale cultivations expressing His_6-rhS100A8 versus wt-rhS100A8. (**B**) Comparison of large-scale cultivations expressing His_6-rhS100A8 versus wt-rhS100A8.

7.3.2 Purification of Recombinant His_6-hS100A8

The soluble proteins from the large-scale cultivation were extracted and purified by affinity chromatography on a cOmplete His-Tag Purification column. Samples were collected from fractions at areas showing high absorbance (*Figure 7.12*) and analysed on a SDS-PAGE gel (*Figure 7.13A*). The gel showed that one-step affinity purification was sufficient to obtain high purity of the His_6-rhS100A8. The bands right above 25 kDa are most probably covalently associated complexes formed due to oxidation. Fractions 14-30 were pooled and the purity of the pooled fractions were analysed on SDS-PAGE (*Figure 7.13B*). The figure is cropped as no other bands were visible (uncropped version in *Appendix IV*). As judged by the gel, the purity is >95%.

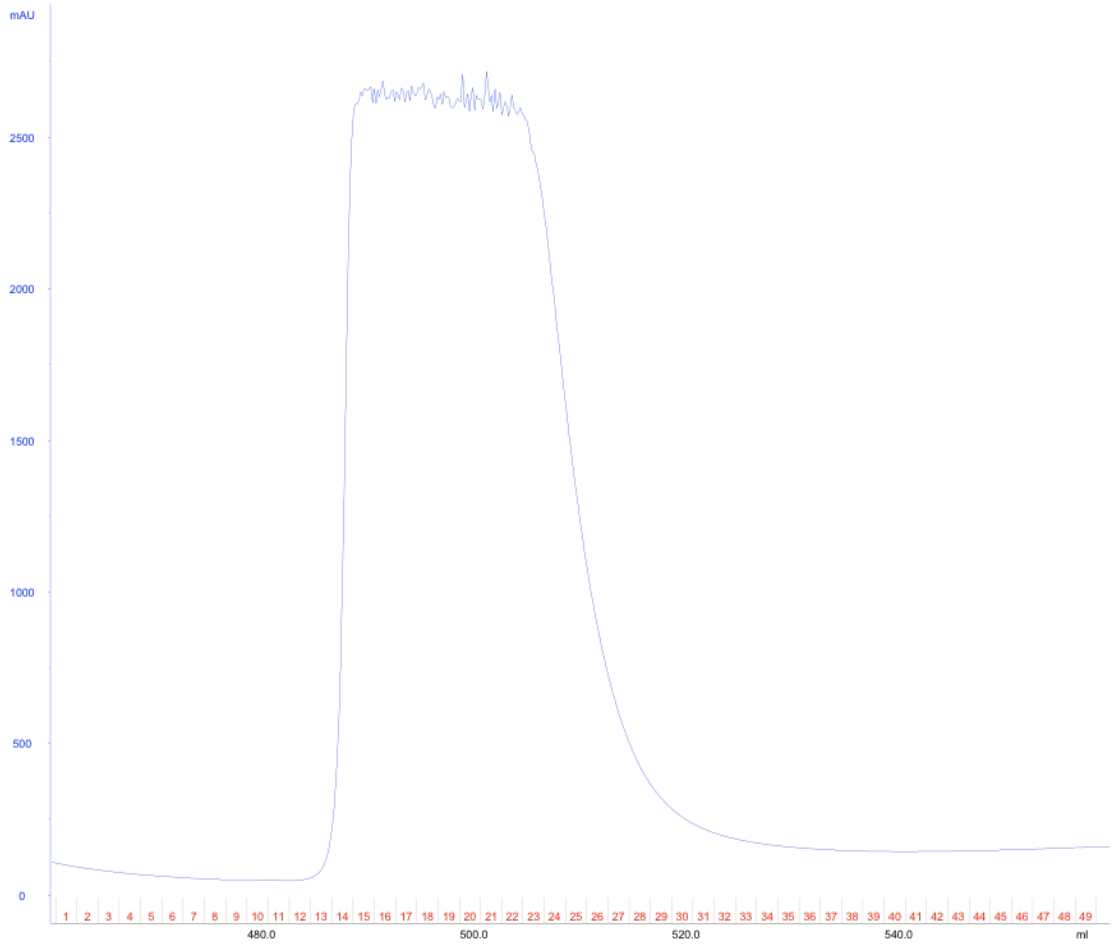

Figure 7.12. Chromatogram of His_6-rhS100A8 purified on a cOmplete His-Tag Purification affinity column. The blue Y-axis and graph shows the UV absorbance at 280 nm (mAU). The X-axis shows volume in mL and the numbers in red are the fraction numbers.

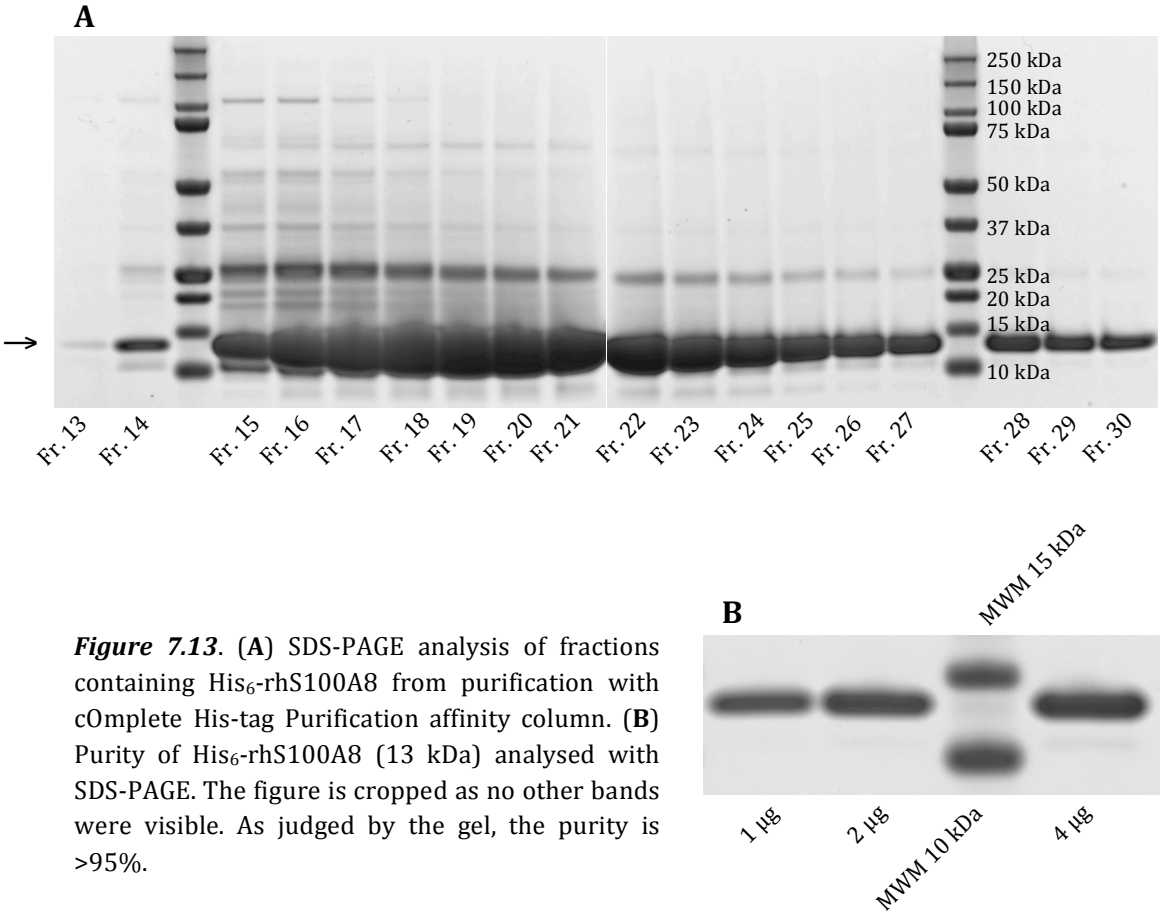

Figure 7.13. (**A**) SDS-PAGE analysis of fractions containing His_6-rhS100A8 from purification with cOmplete His-tag Purification affinity column. (**B**) Purity of His_6-rhS100A8 (13 kDa) analysed with SDS-PAGE. The figure is cropped as no other bands were visible. As judged by the gel, the purity is >95%.

7.4 Cleavage of Recombinant His_6-hS100A8

A small-scale optimization was performed to estimate the appropriate enzyme:target ratio for cleavage. Several concentrations of recombinant enterokinase (rEK), temperatures, buffers and incubation times were tested to optimize the cleavage of His_6-rhS100A8 to remove the His_6-tag.

In the first approach a constant amount of protease (1 U) was added to three different amounts of target protein; 20, 50 and 74 µg (1U/20 µg, 1U/50 µg and 1U/74 µg). The samples were taken after 2, 4, 6, 7, and 16 hours of incubation and analyzed with SDS-PAGE. The gel showed no sufficient cleavage (data not shown).

In the second approach, DTT (reducing agent) was added to the proteins to a final concentration of 10 mM as a precaution to avoid covalently associated complexes when exposed to oxidation. Formations of complexes could in turn form bigger clusters or aggregations, making the enterokinase recognition site

inaccessible. In addition, higher amounts of enterokinase (1, 5 and 10 U) were added to 20 and 50 µg of proteins. Furthermore, the samples were prepared so that the exact same composition could be tested both in room temperature and in 4 °C. The incubation lasted over the weekend and samples were analyzed with SDS-PAGE. A control protein was also loaded on the gel to confirm the activity of the enterokinase. The molecular weight of the uncleaved His_6-rhS100A8 is 13 kDa, and the untagged hS100A8 is 10.8 kDa. As judged by the gel, there is no sufficient cleavage of the target protein (selected data shown in *Figure 7.14A*).

In the third approach, the cleavage buffer was changed to one that lacks $CaCl_2$ as a precaution to avoid formations of higher complexes. The incubation, with enzyme:target ratio 1U/20 µg and 1U/50 µg, lasted for 16 hours in room temperature. Samples were taken and analyzed by SDS-PAGE (selected data shown in *Figure 7.14B*). A control protein was also loaded on the gel to confirm the activity of the enterokinase. As judged by the gel, there is no sufficient cleavage of the target protein.

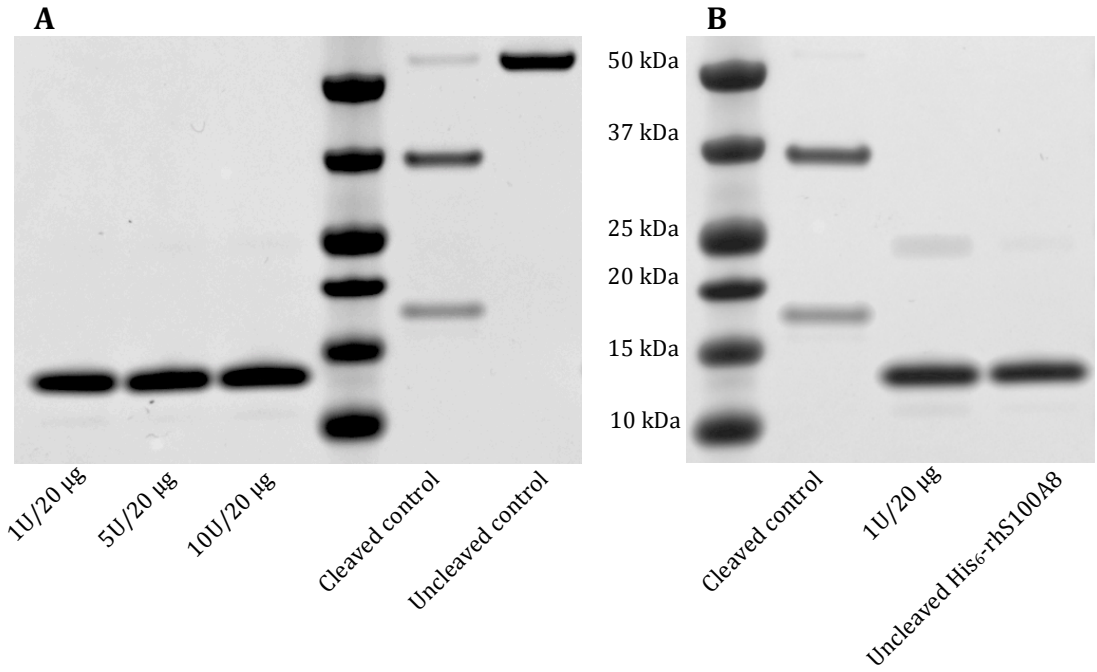

Figure 7.14. (**A**) SDS-PAGE analysis of attempt cleavage of His_6-rhS100A8 with different amounts of rEK. (**B**) SDS-PAGE analysis of attempt cleavage of His_6-rhS100A8 with buffer lacking $CaCl_2$.

7.5 Endotoxin Levels and Protein Concentrations

The recombinant proteins were loaded on a Detoxi-Gel™ Endotoxin Removing Column to reduce the potential endotoxins. A LAL assay was performed to detect and quantify the level of endotoxins. The endotoxin level in His_6-rhS100A8 was determined to be higher than 400 EU/mL, whereas wt-rhS100A8/S100A9 was reduced to 0.1 EU/mL. The endotoxin/protein concentration was calculated to >27 ng endotoxins/mg His_6-rhS100A8 protein and 0.1 ng endotoxin/mg wt-rhS100A8/S100A9 (*Table 7.1*).

Table 7.1. Endotoxin levels of the recombinant proteins before and after Detoxi-Gel™ Endotoxin Removing Column, determined by LAL assay. Endotoxin Unit (EU) is a measure of the activity of the endotoxin.

Protein preparation	**Endotoxin concentration**	**Endotoxin/protein**
His_6-rhS100A8 after column	>400 EU/mL	>27 ng endotoxin/mg protein
wt-rhS100A8/S100A9 after column	0.1 EU/mL	0.1 ng endotoxin/mg protein
wt-rhS100A9 after column	15 EU/mL	3 ng endotoxin/mg protein

The final concentrations of the recombinant proteins were determined by UV adsorption at 280 nm. The final concentrations are presented in *Table 7.2*.

Table 7.2. Protein concentration determined by UV adsorption at 280 nm.

Protein preparation	**Concentration**
His_6-rhS100A8	1.48 mg/mL
wt-rhS100A8/S100A9	0.1 mg/mL
wt-rhS100A9	0.47 mg/mL

7.6 LC-MS

LC-MS was used to determine the exact mass of the recombinant proteins and to analyze the purity. *Figure 7.15A* is a chromatogram of His_6-rhS100A8, showing one peak with an exact mass of 12833. *Figure 7.15B* is a chromatogram of wt-rhS100A8/S100A9, showing two major peaks. The determined exact masses of the rhS100A8 and rhS100A9 subunits are 10835 and 13112 respectively. The LC-MS data of wt-rhS100A9 (*Appendix V*) was used as a reference and exhibits an exact mass of 13112, just like the one of wt-rhS100A9 subunit of the heterodimer complex.

A

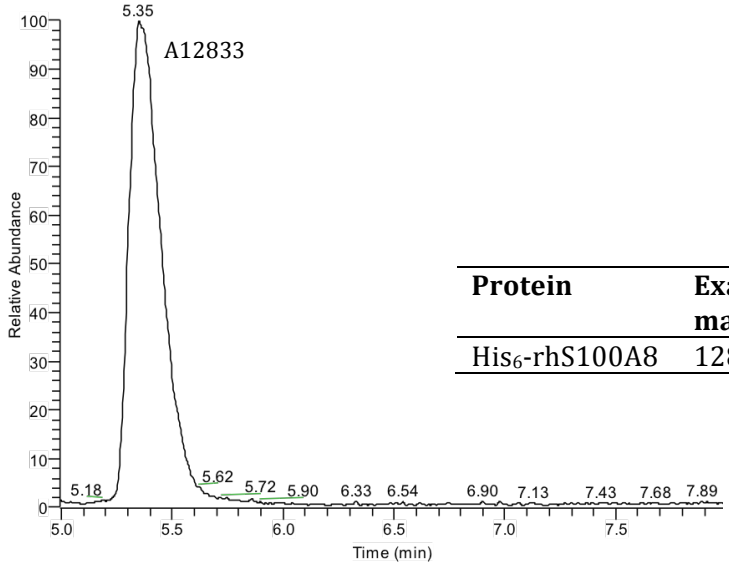

Protein	Exact mass	Theoretical molecular weight
His_6-rhS100A8	12833 Da	12832 Da

B

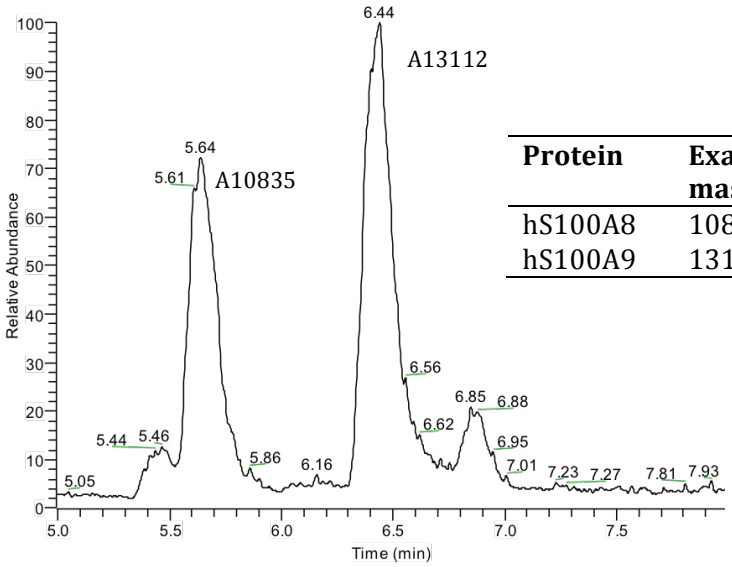

Protein	Exact mass	Theoretical molecular weight
hS100A8	10835 Da	10834 Da
hS100A9	13112 Da	13110 Da

Figure 7.15. (**A**) Chromatogram of His_6-rhS100A8 with an exact mass of 12833 compared to the theoretically calculated mass of 12832 Da. (**B**) Chromatogram of wt-rhS100A8/S100A9. The exact masses of the rhS100A8 and rhS100A9 subunits are 10835 and 13112 respectively compared to the theoretically calculated masses of 10834 Da and 13110 Da.

7.7 Biacore SPR

The bindings of the recombinant S100 proteins with mAbs, human TLR4-MD2 (hTLR4-MD2) and human RAGE (hRAGE) were characterized *in vitro* by surface plasmon resonance studies in Biacore. The concentrations of the recombinant proteins ranged from 3.125-100 nM in experiments with mAbs and from 25-400 nM in experiments with hTLR4-MD2 and hRAGE. Biacore measures the interactions on the chip as response differences (Resp. Diff.) in response units (RU) as a function of time in seconds. The interaction between His_6-S100A8 and mAb 8-5C2 showed approximately 20 times higher response compared to the reference rhS100A8 at a concentration of 50 nM (*Figure 7.16A* and *7.16B*).

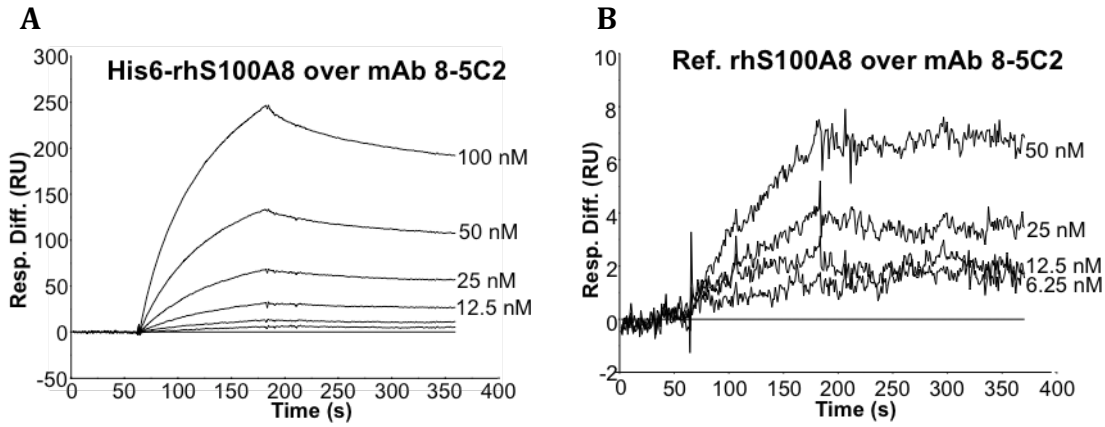

Figure 7.16. Sensorgrams over bindings of recombinant human S100A8 to immobilized mAb 8-5C2. (**A**) shows responses received from His_6-rhS100A8. (**B**) shows responses received from a reference rhS100A8

The sensorgrams presented in *Figure 7.17* show the responses from the interactions between the recombinant proteins and hTLR4-MD2. It was observed that His_6-S100A8 bound to hTLR4-MD2 and when comparing to a reference rhS100A8, displayed 60 times higher response at 400 nM (*Figure 7.17A* and *7.17B*). Lower concentrations of reference rhS100A8 displayed no or very low signals. Regarding the heterocomplex, the reference protein (a non-recombinant hS100A8/S100A9 purified from granulocytes) displayed three times higher responses than rhS100A8/S100A9 at 400 nM, whereas the rest of the concentrations of rhS100A8/S100A9 displayed no or very low signals (*Figure 7.17C* and *7.17D*). In contrast, the homocomplex wt-rhS100A9, used as a reference to the heterocomplex, displayed higher signals (*Figure 7.17E*).

The sensorgrams presented in *Figure 7.18* show the responses from interactions between the recombinant proteins and hRAGE. Also here, it was observed that His_6-S100A8 bound to hRAGE with much higher responses than compared to the reference rhS100A8, with more than 150 times higher responses at 400 nM (*Figure 7.18A* and *7.18B*). Lower concentrations of reference rhS100A8 displayed

no or very low signals. In *Figure 7.18C* and *7.18D*, the sensorgrams show that wt-rhS100A8/S100A9 did not bind to hRAGE whereas the reference hS100A8/S100A9 displayed only binding at 400 nM. In contrast, the homocomplex wt-rhS100A9, used as a reference to the heterocomplex, displayed higher signals (*Figure 7.18E*).

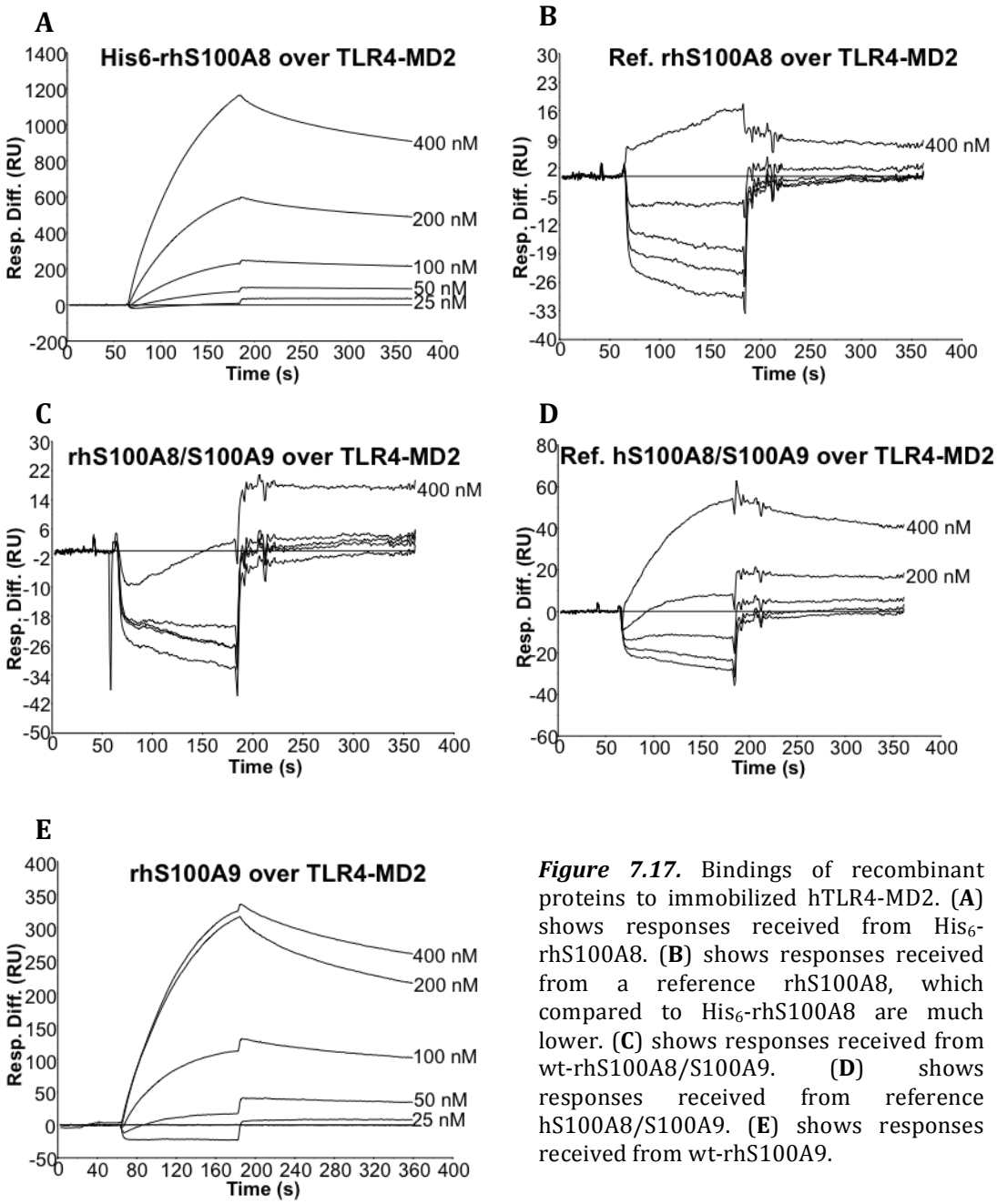

Figure 7.17. Bindings of recombinant proteins to immobilized hTLR4-MD2. (**A**) shows responses received from His_6-rhS100A8. (**B**) shows responses received from a reference rhS100A8, which compared to His_6-rhS100A8 are much lower. (**C**) shows responses received from wt-rhS100A8/S100A9. (**D**) shows responses received from reference hS100A8/S100A9. (**E**) shows responses received from wt-rhS100A9.

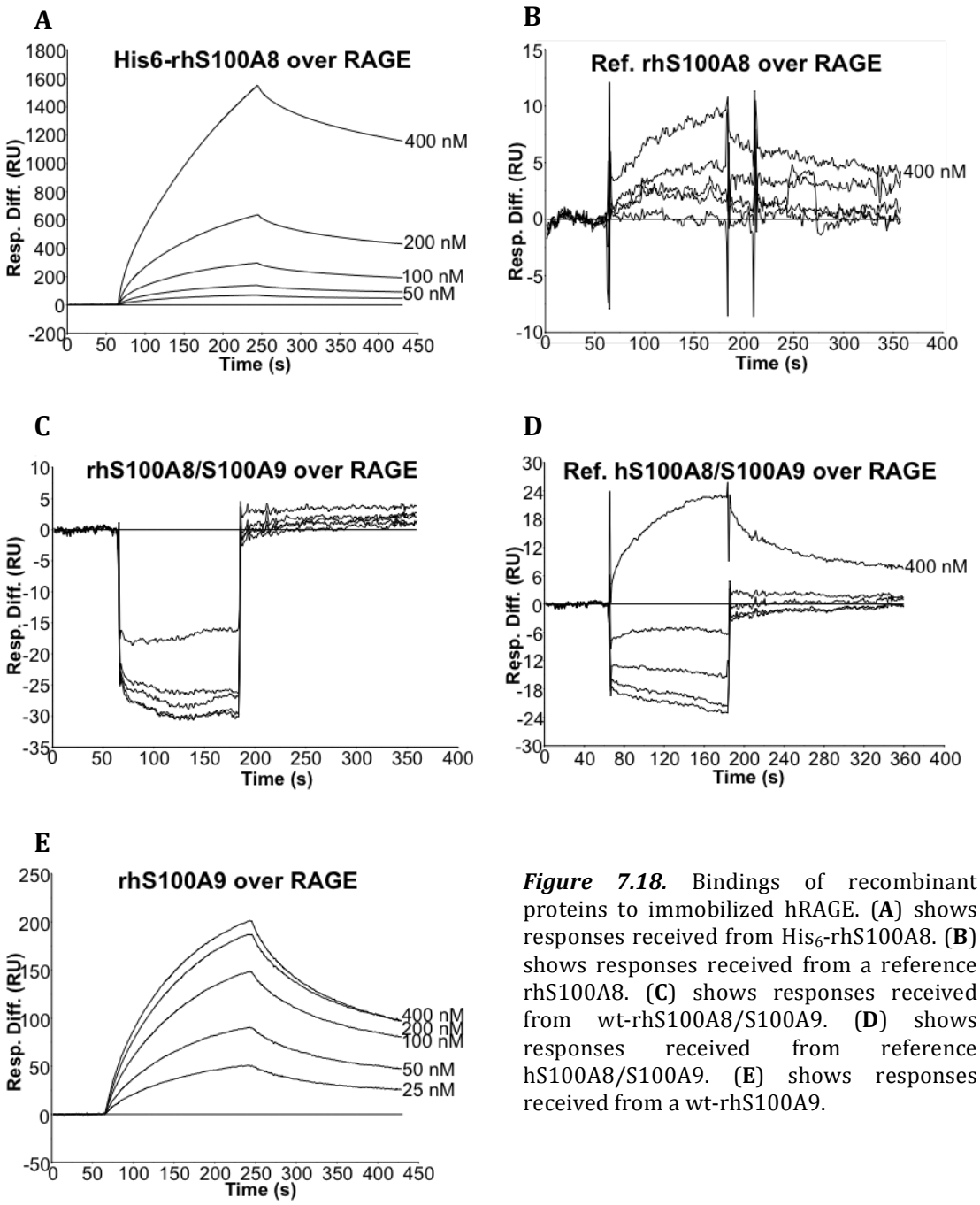

Figure 7.18. Bindings of recombinant proteins to immobilized hRAGE. (**A**) shows responses received from His_6-rhS100A8. (**B**) shows responses received from a reference rhS100A8. (**C**) shows responses received from wt-rhS100A8/S100A9. (**D**) shows responses received from reference hS100A8/S100A9. (**E**) shows responses received from a wt-rhS100A9.

7.8 NF-κB Luciferase Reporter Assay

The NF-κB Luciferase reporter assay was used to characterize the recombinant proteins in terms of activating the signalling pathway of NF-κB via the TLR4 receptors in a cell-based *in vitro* system. The assay measures the luminescence as a result of catalysed luciferins (substrate) in response light units (RLU). Samples of His_6-rhS100A8 were tested in the assay at concentrations of 0.4 and 0.15 μM, whereas samples of wt-rhS100A8/S100A9 were tested at 0.4 and 2 μM. 100 μL of each recombinant protein solution at different concentrations were sampled into an optiplate with cells, and amounts of contaminating endotoxins found in each protein concentration are presented in *Table 7.3*.

Table 7.3. The amount of endotoxins present in each protein sample in the NF-κB Luciferase reporter assay experiment.

Protein preparation	Concentration	Endotoxin (pg)
His_6-rhS100A8	0.4 μM	>28
	0.15 μM	>11
wt-rhS100A8/S100A9	0.4 μM	0.096
	2 μM	0.48
wt-rhS100A9	0.4 μM	3.2
	0.15 μM	1.2

The responses from incubation of each protein sample are presented in *Figure 7.19A*. The diagram indicates that there is activity present in the His_6-rhS100A8 protein samples, higher than the ones of the reference rhS100A8 at both 0.4 and 0.15 μM.

In *Figure 7.19B*, the data over wt-rhS100A8/S100A9 shows higher responses in comparison to the reference protein (a non-recombinant hS100A8/S100A9 purified from granulocytes). Neither 0.4 μM nor 2 μM of the reference protein gave any responses whereas the wt-rhS100A8/S100A9 showed 660 and 2300 RLU respectively. In contrast, the homocomplex wt-rhS100A9, used as a reference, displayed higher signals (*Figure 7.18E*).

A control was also sampled in a well containing LPS (endotoxin) in a concentration of 50 pg/mL (5 pg LPS/well).

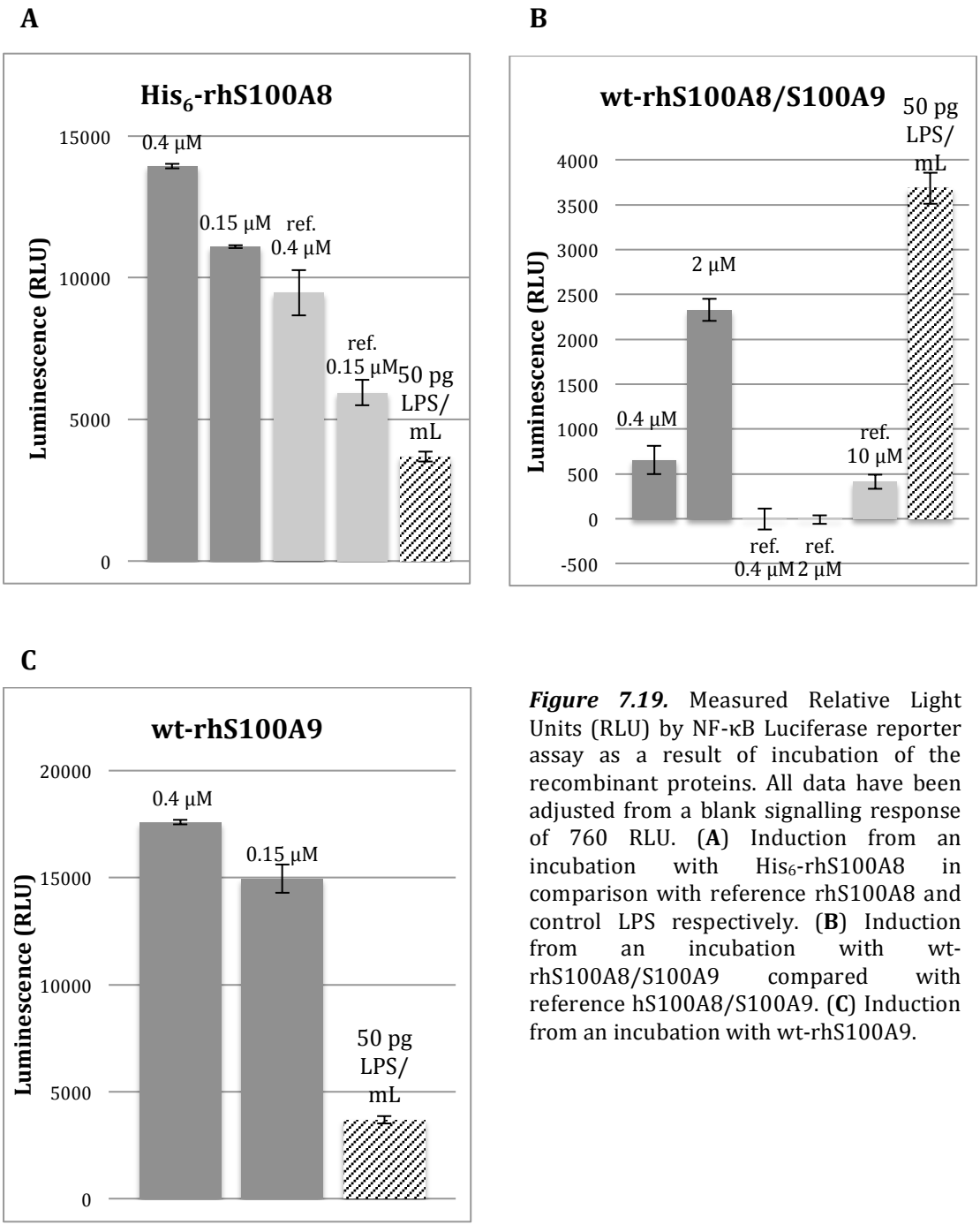

Figure 7.19. Measured Relative Light Units (RLU) by NF-κB Luciferase reporter assay as a result of incubation of the recombinant proteins. All data have been adjusted from a blank signalling response of 760 RLU. (**A**) Induction from an incubation with His_6-rhS100A8 in comparison with reference rhS100A8 and control LPS respectively. (**B**) Induction from an incubation with wt-rhS100A8/S100A9 compared with reference hS100A8/S100A9. (**C**) Induction from an incubation with wt-rhS100A9.

Chapter 8

Discussion

The S100A8 and S100A9 proteins have become the focus of many current researches due to their association with numerous human diseases. Both S100A8 and S100A9 belong to the DAMP family and they promote inflammatory responses during infections, allergies and autoimmune diseases (Chan *et al*., 2012). However, the initial events during protein binding to DAMP receptors, such as TLR4 and RAGE, are not yet clear. The focus of this master's project was to produce recombinant human S100A8 and S100A9 to further characterize their interactions with TLR4-MD2 and RAGE. Active Biotech have previously produced and characterized recombinant human S100A9. Hence, one of the project aims was mainly to find a suitable strategy to produce human S100A8. An ambition was also to use the produced rhS100A8 to form heterocomplexes with produced rhS100A9 and essentially also test their binding activities.

8.1 Stability of Recombinant Human S100A8

In the first approach to produce recombinant human S100A8, the proteins were expressed in its wild-type form. In testing of the expression, a small-scale cultivation was performed and the expressed fractions of soluble and insoluble proteins were identified with Western blot. The blot revealed a faint band below the 10 kDa MWM in one sample containing soluble proteins taken 3 hours after induction. However, the blot still developed a band correlating to S100A8-derived molecules and recognized with anti-hS100A8 antibodies. The molecular weight of this portion was less than 10.8 kDa, hence it is thereby likely that the faint band shows fragmentations of the soluble protein.

It is widely known that S100A8 is extremely prone to oxidation (Lim *et al*., 2009); hence DTT (a reducing agent) was added in each step of the experimental procedures as a precaution. The overall experience with S100A8 was that it was extremely instable, especially in its soluble form despite the presence of DTT. Apart from what could be seen in the Western blot, many other signs suggest that the protein becomes fragmented even when exposed to air. For example, the soluble proteins seemed to disappear during the purification procedure, as detected by SDS-PAGE and Western blot. In each purification step, the protein solution is exposed to air almost an entire working day. If the protein solution requires additional purification steps, the air exposure might be too extensive. In addition, the protein solutions had to be kept in the fridge during the non-

working hours and even there they were exposed to air. Freezing the proteins is not a good alternative as cycles of freeze-thaws results in protein instability. Due to the change of environment, it could result in aggregation, precipitation, loss of activity etc.

The long purification procedure might be the reason the soluble proteins were barely visible on the SDS-PAGE gel after the second purification column and not even detectable on a Western blot. If fragments already could be detected in the small-scale cultivation, a weekly long procedure with extraction and purification was a risk for further fragmentations. Another reason could be major protein loss after the second purification step (*Appendix II*), or it could be a combination of both.

As S100A8 and S100A9 have become the focus of many current researches, they seem to exhibit different functions in biology; they have pro- and anti-inflammatory properties; may promote would-healing; play a central role as DAMPs; are involved in restoring homeostasis etc. A proposal made by Lim et al. in 2011, suggests that especially S100A8 also acts as oxidant scavengers in the body. This could be applied to what could be observed here. It is known that proteins (in general) that are target of free radicals are subject to fragmentation and denaturation (Bourdon and Blache, 2001). Based on these remarks, the hypothesis is that S100A8 is physically constructed to help protecting the tissues against oxidative damages by acting as oxidant scavengers (as one of its many biological roles), and the effect is that they become degraded due to oxidation. The hypothesis is encouraged by the observations made by Active Biotech when they studied the heterodimer complex of S100A8 and S100A9. They suggest that it might be only the S100A9 part of the heterodimer complex that contributes to cell signalling (Unpublished data). Based on this, one theory is that S100A8 and S100A9, which are up-regulated as heterodimer complexes at sites of inflammation, have different roles – the S100A8 is there to act as a oxidant scavenger and the S100A9 is the one contributing to cell signalling via receptors, either as a subunit (after S100A8 is fragmented or dissociated) or as part of the heterodimer complex. However, this theory does not rule out the possibility that S100A8 as a homodimer can contribute to cell signalling via receptors in other biological roles.

The solubilized proteins from the insoluble fraction were found to be less unstable, however, the procedure with refolding and purification was challenging. During refolding, there were major aggregations in the dialysis tube, which was probably due to poor choice of methods, especially for S100A8. In addition, the purification also resulted in further loss of the proteins. Hence, it was decided to not continue working with wt-rhS100A8 neither from the soluble nor the insoluble fraction since the final production yields were too low.

8.2 Recombinant His_6-rhS100A8

In the second approach to produce the recombinant human S100A8, the proteins were expressed with a His_6-tag. The cultivation strategy and parameters were the same used to express wt-rhS100A8. At 3 hours after induction, the OD_{620} for expression of wt-rhS100A8 was much higher than the one for His_6-rhS100A8, however at 21 hours after induction, they both land at approximately 5.5 in OD. The low OD seen in the beginning of the cultivation for the expression of His_6-rhS100A8, is however as expected. As could be seen from the SDS-PAGE analysis of smalls-scale cultivation, His_6-rhS100A8 was highly expressed. A high expression of proteins correlates to a slower growth rate of the *E. coli*, as more energy is used for the production of proteins rather than for proliferation. Despite the fact that the SDS-PAGE gel showed higher protein expression in its insoluble form, the decision was to perform large-scale cultivation to express soluble proteins. The reason was that there were sufficient amounts of soluble proteins to work with and the time-consuming denaturing/refolding processes would be avoided.

The experience with His_6-rhS100A8 was overall very positive. The one-step purification of His_6-rhS100A8 was fast, easy and efficient. The protein seemed to be stabilized when fused to the His-tag, although there are no good explanation why this is the case. One speculation could be that the His_6-tag is shielding the N-terminal of the protein. If the N-terminal of the protein is involved in the role as an oxidant scavenger, it could be that fusing the His_6-tag to its N-terminal may suppress the oxidant scavenger-activity and hence making it less prone to fragmentation. On the contrary, the His_6-tag might instead protect the S100A8 from oxidation. As reviewed in Lim *et al*., (2011), histidine residues are particularly susceptible to oxidation by ROS. Thus the six histidine in tandem might be protecting S100A8 by taking care of ROS or protect the S100A8 from other forms of oxidation.

Nevertheless, as any other protein with cysteine in their amino acid sequence, the His_6-rhS100A8 was still able to form covalently associated homodimers via disulphide bonds, possibly as a result of oxidation (visible on SDS-PAGE gel at 26 kDa). As confirmed by Vogl *et al*., the expressed S100A8 and S100A9 require formation of non-covalently associated complexes in order to exhibit biological activities *in vivo* and *in vitro* (Vogl *et al*., 2006). In order to reduce oxidation, the His_6-rhS100A8 proteins were exposed to nitrogen gas and stored in 1 mM DTT (reducing agent). The final purity and product yield of the His_6-rhS100A8 were high and promising. In addition, LC-MS analysis of the protein revealed that the exact mass is 12833, which can be considered close to the theoretically calculated molecular weight of 12832 kDa. Note that the molecular weight is an average of the molecular weight for all the molecules with different isotopic compositions.

8.2.1 Cleavage of His_6-rhS100A8

The attempts to cleave off the tag from His_6-rhS100A8 were unsuccessful and far more challenging than expected, seeing as the vector construct looked optimistic. When the first attempt failed, the second attempt had DTT added to the protein solution to a final concentration to 10 mM. The reason for adding DTT was that it was assumed that the failure could be due to formations of covalently associated complexes when exposed to air. Such formations could in turn form bigger clusters or aggregations, making the enterokinase recognition site inaccessible. Failure of the second approach lead to the decision to change the buffer to one that lacks $CaCl_2$. The choice of changing the buffer was, also here, because of the assumption that the failure might be due to complex formations of higher orders. Even after adding more DTT and changing the buffer, the His-tag could still not be cleaved off, dismissing the assumptions above. It could be that the His-tag is shielding the recognition site or that the buffers used were not optimal.

8.3 Heterodimer Complex

Simply mixing recombinant expressed subunits (soluble proteins) has shown to be an insufficient way of producing S100A8/S100A9 heterodimers with proper complex formation. Vogl *et al*. confirmed this in 2006 where they observed that there were no significant interactions between the subunits. With this information in mind, the strategy was to extract insoluble proteins of S100A8 and S100A9 and later allow them to naturally fold and associate as heterodimers during the denaturing and refolding processes.

In parallel to the production of homodimeric wt-rhS100A8, the insoluble fraction of wt-rhS100A8 was used to form heterodimer complex with the insoluble fraction of wt-rhS100A9. In contrast to wt-rhS100A8, the wt-rhS100A9 was found both stable and easy to purify. The first purification step of heterodimer complexes showed visible bands on the SDS-PAGE gel that correspond to 10.8 and 13.2 kDa in few of the fractions. A second purification step was considered, however, having the experience with wt-rhS100A8 purification in mind, it could be a risk that a second step would result in loss of proteins. Hence, the decision was to use the purest fraction containing the heterodimer complex. LC-MS analysis of the heterodimer complex revealed that the exact masses of S100A8 and S100A9 are 10835 and 13112 respectively. Compared to the theoretical molecular weights of 10834 and 13110 kDa they are fairly close.

8.4 Endotoxin Levels

Following the purification, the recombinant proteins had to undergo an endotoxin removal step and to have their concentrations determined. It is necessary to determine the endotoxin levels prior to the NF-κB Luciferase

reporter assay to ensure that the received responses are not contributed by endotoxins, but since the time-schedule could not allow it, the quantity was determined afterwards. A LAL assay was used to detect and quantify the endotoxin levels. The assay revealed that the His_6-rhS100A8 had >27 ng endotoxin/mg protein. The cause was likely due to protein (and hence also endotoxin) overload of the Detoxi-Gel™ Endotoxin Removing Columns. The overload resulted in saturation of the columns and the endotoxins could therefore not be reduced any further in a single step. The endotoxin removal of wt-rhS100A8/S100A9 was a lot more successful and reduced to 0.1 ng endotoxin/mg protein.

8.5 Binding activities of His_6-rhS100A8

The NF-κB Luciferase reporter assay was used to characterize the recombinant proteins in terms of activating the signalling pathway of NF-κB via the TLR4-MD2 receptors. Prior to the assay, the recombinant proteins underwent an endotoxin removal step to rule out any endotoxin contaminations that could have contributed to extra response in the reporter assay. However, the LAL assay detected high levels of endotoxin in the His_6-rhS100A8 batch. The responses received from the NF-κB Luciferase reporter assay indicated that there were binding activities of His_6-rhS100A8 to TLR4 in cell-based *in vitro* system, however if it is the protein, the endotoxins or a combination of both that are responsible for the activity remains questionable. A sample containing 5 pg of LPS (endotoxin) was also tested on the NF-κB Luciferase reporter assay, giving a response of approximately 3700 RLUs. With an amount of >28 pg endotoxin in the 0.4 μM His_6-rhS100A8 sample and >11 pg in the 0.15 μM, it is obvious that the amount of endotoxin levels of this batch were too high to rule out any responses contributed by endotoxins. Nevertheless, the reference rhS100A8 (detoxified) gave good response, between 50-70% of the response given by His_6-rhS100A8. Similar interactions between rhS100A8 and TLR4 were observed in studies conducted by Vogl *et al*. in 2007 and Fassl *et al*., 2015, using HEK293 cells stably transfected with human TLR4, CD14 and MD2 genes. Their protein batches contained ~ 0.7 ± 0.5 pg LPS/ μg protein and <1 pg LPS/μg protein respectively. Since they could confirm that rhS100A8 exhibit interactions with TLR4, it suggests that the responses received from His_6-rhS100A8 might not be fully contributed by endotoxins only but also from the protein itself. Reducing the endotoxin levels and testing with the assay again could only verify this.

The *in vitro* binding interactions between His_6-rhS100A8 and TRL4-MD2 could also be observed with SPR studies on Biacore. Compared to the reference rhS100A8, His_6-rhS100A8 exhibited 60 times higher RUs at 400 nM. Similar observation could be seen when bound to RAGE. The His_6-rhS100A8 gave 150

times higher responses at 400 nM than compared to the one given by reference wt-rhS100A8.

The difference in RUs might be due to higher stability of the His_6-rhS100A8. Responses contributed by endotoxins are highly unlikely as SPR studies are not as sensitive to endotoxins as NF-κB Luciferase reporter assay. The responses given by SPR studies are based on concentration and mass over time. With high concentrations of recombinant protein in the batch, it is highly unlikely that the observed responses are contributed by endotoxins. Similar interactions between rhS100A8 and TLR4-MD2 were observed in a study conducted by Vogl *et al*. in 2007, apart from that they characterized bindings of TLR4-MD2 with immobilized rhS100A8 on the sensor chip instead of the other way around. They could observe responses by TLR4-MD2 at concentrations of 67 and 121 nM. In considerations of RAGE, Björk *et al*. (2009) confirmed that binding of S100A8 to RAGE in SPR studies was negligible, in contrast to human S100A8/S100A9, which exhibit interactions. The high responses received from His_6-rhS100A8 could either be contributed by the His-tag itself or it could have stabilized the rhS100A8 to interact with RAGE. Since Biacore SPR measurement are based on mass and concentration, another more reasonable explanation is that His_6-rhS100A8 have formed larger complexes as 5 mM Ca^{2+} and 150 μM Zn^{2+} were present in the buffer. In comparison to the recombinant wt-S100A8 used in the study conducted by Björk *et al*. (2009) and the reference wt-rhS100A8, they might have lost their activity due to e.g. instability and structural modifications caused by oxidation.

In another SPR experiment, the binding interactions between His_6-rhS100A8 and its corresponding mAb were tested. The given data showed higher responses for His_6-rhS100A8 than compared to the one for reference rhS100A8. Again, the assumption is that the His_6-tag stabilizes the proteins and helps them retaining their structures, whereas the reference rhS100A8 simply does not have high binding activities due to e.g. potential oxidative modifications in the structure, or else the mAb would have recognized it as an antigen.

8.6 Binding activities of wt-rhS100A8/S100A9

The data over wt-rhS100A8/S100A9 in the NF-κB Luciferase reporter assay indicated that there were cell-based *in vitro* binding activities present at 0.4 and 2 μM whereas no responses could be detected for the reference hS100A8/S100A9 at the same concentrations. At 10 μM the reference hS100A8/S100A9 gave a response although lower than the one of wt-rhS100A8/S100A9 at 0.4 μM. With as little as 1 pg endotoxins in the wt-rhS100A8/S100A9 batch, the contribution by endotoxins to the responses can be ruled out. One reason the data differentiate from one another could be that the

reference hS100A8/S100A9, which is purified from granulocytes, has lower biological activity than recombinantly expressed S100A8, due to e.g. instability or structural modifications. Another reason could be that the RAGE receptors on cells are structurally different after post-transcriptional modifications compared to the RAGE receptors immobilized on the sensor chip used in the SPR experiments.

In SPR experiments with wt-rhS100A8/S100A9, the sensorgrams showing binding interactions with hTLR4-MD2 indicates that the responses are poor. Only at 400 nM showed binding activities. The responses received by the reference hS100A8/S100A9 showed binding at 200 and 400 nM, which were slightly higher than wt-rhS100A8/S100A9. In experiments with hRAGE, the wt-rhS100A8/S100A9 did not exhibit any responses within the concentration frame (25-400 nM) whereas the hS100A8/S100A9 exhibited poor responses at 400 nM. The reason why interactions exists in the NF-κB Luciferase reporter assay but not the SPR studies could be that NF-κB Luciferase reporter assay used much higher concentrations (compare μM to nM). A contrast can also be seen in experiments with wt-rhS100A9 and reference rhS100A8, which showed high binding signals. This suggests that S100A8 and S100A9 have high biological activities as homocomplexes, but when S100A8 and S100A9 exist as heterocomplex, the binding activities seem to be drastically decreased.

The low/non-existing responses from wt-rhS100A8/S100A9 were however anticipated. In biology, the complex has shown to be up-regulated in response to stress (Mørk *et al*., 2003; Ross and Herzberg, 2001). In a study conducted by Foell *et al.* in 2010 showed that the concentration of S100A8/S100A9 complexes in blood serum is superior over conventional biomarkers in patients. Based on the study, a speculation is that the excess amount of the complex ends up in the blood stream mostly in a latent state. Since the concentration of S100A8/S100A9 complexes in blood serum is high, if they all would have been active, they would have initiated several cell signaling at the same time, which would have been devastating for the human being. The reason these binding responses can be seen in both Biacore and in NF-κB Luciferase reporter assay is that abnormally high concentrations of the complex were used. In the study conducted by Foell *et al.* in 2010, they discovered as much as 30 nM (=715 ng/mL) in the blood serum in patients, compared to the concentrations of 200-400 nM that gave signals in Biacore and 0.4-2 μM in the NF-κB Luciferase reporter assay. In addition, the numbers of receptors on the chip and on the HEK293 cell surface are highly abundant and abnormal (despite being accepted models), which increases the possibility and prevalence of interactions. In combination with the theory proposed by Active Biotech about the activity of S100A9, a question should also be aroused to whether the heterocomplex actually are active DAMPs or if the roles are played by homocomplexes only.

Chapter 9

Future Prospects

The experiences with wt-rhS100A8 and His_6-rhS100A8 are that the latter has shown to be more superior in terms of expression, purification and protein stability. The recommendation is to continue working with His_6-rhS100A8. However, the endotoxin levels of the His_6-rhS100A8 protein solution need to be strictly controlled and reduced down to <1 EU/mL. A recommendation is to add additional repeats or avoid overloading by using several columns in parallel. The purification of His_6-rhS100A8 is both fast and easy, hence a suggestion is also to consider adding a second purification step with the same affinity column in order to decrease the endotoxin levels further, prior to the endotoxin removal. In addition, extending the time of washing before elution is also recommended in order to wash out as much endotoxins as possible. The downside is that there might be some protein loss as a result of adding an extra step.

In order to verify that the binding activities seen in the cell-based *in vitro* system are solely contributed by the protein and not by endotoxins, the detoxified protein should be tested again with NF-κB Luciferase reporter assay. Another way of measuring the activation of the NF-κB signalling pathway should also be considered. For example qRT-PCR analysis of mRNA expressions of certain proteins could be performed. Proteins such as TNF-α, IL-8, IL-6 and MCP-1 are expressed in response to the activation of the NF-κB signalling pathway. By measuring the abundance of mRNA expression for these proteins, it could be used to measure the activation of NF-κB signalling pathway.

Future prospects should also consider investigating other methods to cleave off the His-tag from His_6-rhS100A8. A recommendation is to try cleaving the protein in parallel to the purification step, i.e. instead of eluting the protein, cleavage can be performed when the proteins are adhered to the affinity column. This might help the protein to expose the enterokinase recognition site and prevent protein clustering. An alternative is to modify the cleavage buffers and investigate other recombinant enterokinases. Supplier such as Merck, Sigma Aldrich and Life Technologies provide other recombinant enterokinases that can be tested.

When a successful method of cleavage has been found, further investigations need to consider performing the same characterization experiments with the cleaved protein included, in order to verify that the results generated by this

project was not contributed by the His_6-tag itself. Heterodimer complexes of wt-rhS100A9 with His_6-rhS100A8 or its cleaved form could also be the next approach to study the binding activities of the heterodimer complex.

Chapter 10

Conclusion

S100A8 and S100A9 have become the focus of many current researches since they seem to play a central role as DAMPs, however the initial events during protein binding to its receptors are not yet clear. To study their binding activities to DAMP receptors, rhS100A8 and rhS100A9 were produced. The production of rhS100A8 was expressed in its wild-type form and fused to a His_6-tag, with the latter showing to be more superior in terms of expression, purification and protein stability. The wt-rhS100A8 seemed to have very low stability, which is probably due to oxidation. The final production yield was significantly higher for His_6-tagged rhS100A8 as the wild-type form could not be purified without major protein loss. LC-MS also revealed an exact mass that is close to the theoretical molecular weight. However, attempts to cleave off the tag were unsuccessful and far more challenging than expected. The cause of protein stability with the aid of His_6-tags is however unclear and needs further investigation to clarify.

Formation of heterocomplexes from insoluble wt-rhS100A8 and insoluble wt-rhS100A9 were performed with denaturing and refolding processes to obtain solubilized heterocomplexes. The LC-MS revealed exact masses closely correspond to the theoretical molecular weights. However, the final production yield was low as only a small fraction after the first purification step was used as the finalized protein solution.

This study has demonstrated that recombinant human S100A8 tagged to a His_6-tag has exhibit high responses *in vitro* with SPR studies when screening for interactions with TLR4-MD2 and especially RAGE, which has previously not been confirmed. Additionally, recombinant wild-type human S100A8 in complex with S100A9 have also exhibit biological activities in cell-based *in vitro* system at high concentrations. The His_6-tagged rhS100A8 have also shown activities in cell-based *in vitro* systems, although the data are highly questionable due to the likelihood of endotoxin influences. Morover, data over binding activities of homo- versus heterocomplexes confirmed that S100A8 and S100A9 have high biological activities as homocomplexes, but when S100A8 and S100A9 exist as heterocomplex, the binding activities seem to be drastically decreased.

References

Arai, K., Teratani, T., Nozawa, R. and Yamada, T. (2001) *Immunohistochemical investigation of S100A9 expression in pulmonary adenocarcinoma: S100A9 expression is associated with tumor differentiation.* Oncol Rep 2001;8(3):591–6.

Baneyx, F. (1999) *Recombinant protein expression in Escherichia coli.* Curr. Opin. Biotechnol. 10, 411–421. doi: 10.1016/S0958-1669(99)00003-8

Bianchi, M.E. (2007) *DAMPs, PAMPs and alarmins: All we need to know about danger*. J. Leukoc. Biol. **2007**, 81, 1–5.

Björk, P., Björk, A., Vogl, T., Stenström, M., Liberg, D., Olsson, A., Roth, J., Ivars, F. and Leanderson, T. (2009) *Identification of human S100A9 as a novel target for treatment of autoimmune disease via binding to quinoline-3-carboxamides*. PLoS Biol. **2009**, *7*, doi:10.1371/journal.pbio. 1000097.

Bourdon, E. and Blache, D. *The importance of proteins in de- fense against oxidation*. Antioxid Redox Signal 3: 293–311, 2001.

Boyd, J.H., Kan, B., Roberts, H., Wang, Y. and Walley, K.R. (2008) *S100A8 and S100A9 mediate endotoxin-induced cardiomyocyte dysfunction via the receptor for advanced glycation end products*. Circ. Res. **2008**, *102*, 1239–1246.

Buckley, T. and Ehrhardt, C. (2009) *The Receptor for Advanced Glycation End Products (RAGE) and the Lung.* Hindawi Publishing Corporation Journal of Biomedicine and Biotechnology Volume 2010, Article ID 917108, 11 pages doi:10.1155/2010/917108

Carlsson, H., Petersson, S. and Enerback, C. *Cluster analysis of S100 gene expression and genes correlating to psoriasin (S100A7) expression at different stages of breast cancer development.* Int J Oncol 2005;27(6):1473–81.

Chan, J. K., J. Roth, J. J. Oppenheim, K. J. Tracey, T. Vogl, M. Feldmann, N. Horwood, and J. Nanchahal. (2012) *Alarmins: awaiting a clinical response*. J. Clin. Invest. 122: 2711–2719.

Chant, A., Kraemer-Pecore, C. M., Watkin, R., and Kneale, G. G. (2005*). Attachment of a histidine tag to the minimal zinc finger protein of the Aspergillus nidulans gene regulatory protein AreA causes a conformational change at the DNA-binding site.* Protein Expr. Purif. 39, 152–159. doi: 10.1016/j.pep.2004.10.017

Chauvin, S. (2011) Updated by Yin, C. (2012) *NF-κB Luciferase Assay.* Retrieved 2015-06-12 from http://www.bowdish.ca/lab/wp-content/uploads/2012/07/NF-KB-Luciferase-Assay-Protocolv2.pdf

Cheng, P., Corzo, C.A., Luetteke, N., Yu, B., Nagaraj, S., Bui, M.M., Ortiz, M., Nacken, W., Sorg, C., Vogl, T.; *et al*. (2008) *Inhibition of dendritic cell differentiation and accumulation of myeloid-derived suppressor cells in cancer is regulated by S100A9 protein*. J. Exp. Med. **2008**, 205, 2235–2249.

Cross, SS., Hamdy, FC., Deloulme, JC. and Rehman, I. *Expression of S100 proteins in normal human tissues and common cancers using tissue microarrays: S100A6, S100A8, S100A9 and S100A11 are all overexpressed in common cancers.* Histopathology 2005;46(3):256–69.

del Solar, G., and Espinosa, M. (2000) *Plasmid copy number control: an ever-growing story.* Mol. Microbiol. 37, 492–500. doi: 10.1046/j.1365- 2958.2000.02005.x

Egan, L. J. and Toruner, M. (2006) *NF-κB Signaling: Pros and Cons of Altering NF-κB as a Therapeutic Approach*. 2006; Ann. N.Y.

Ehrchen, J.M., Sunderkotter, C., Foell, D., Vogl, T. and Roth, J. (2009) *The endogenous Toll-like receptor 4 agonist S100A8/S100A9 (calprotectin) as innate amplifier of infection, autoimmunity, and cancer*. J. Leukoc. Biol. **2009**, 86, 557–566.

El-Rifai, W., Moskaluk, CA., Abdrabbo, MK., Harper, J., Yoshida, C., Riggins, GJ., *et al.* (2002) *Gastric cancers overexpress S100A calcium-binding proteins.* Cancer Res 2002;62(23):6823–6.

Fahnert, B., Lilie, H. and Neubauer, P. (2004) *Inclusion bodies: formation and utilization.* Adv Biochem Eng/Biotechnol 89: 93–142.

Foell, D., Wittkowski, H., Ren, Z., Turton, J., Pang, G., Daebritz, J., Ehrchen, J., Heidemann, J., Borody, T., Roth, J., Clancy, R. (2008) *Phagocyte-specific S100 proteins are released from affected mucosa and promote immune responses during inflammatory bowel disease*. J. Pathol. **216,** 183–192.

Gabrilovich, D.I. and Nagaraj, S. (2009) *Myeloid-derived suppressor cells as regulators of the immune system*. Nat. Rev. Immunol. **2009**, *9*, 162–174.

Ghavami, S., Rashedi, I., Dattilo, B.M., Eshraghi, M., Chazin, W.J., Hashemi, M., Wesselborg, S., Kerkhoff, C. and Los, M. (2008) *S100A8/A9 at low concentration promotes tumor cell growth via RAGE ligation and MAP kinase-dependent pathway*. J. Leukoc. Biol. **2008**, *83*, 1484–1492.

Goyette J., Geczy, CL. (2011) *Inflammation-associated S100 proteins: new mechanisms that regulate function*. Amino Acids 41: 821–842.

Graumann, K., and Premstaller, A. (2006) *Manufacturing of recombinant therapeutic proteins in microbial systems*. Biotechnol. J. 1, 164–186. doi: 10.1002/biot.200500051

Guzzetta, A (2001) *Reverse Phase HPLC Basics for LC/MS*. Retrieved 2015-06-12 from http://www.ionsource.com/tutorial/chromatography/rphplc.htm

Hermani, A., de Servi, B., Medunjanin, S., Tessier, P.A. and Mayer, D. (2006) *S100A8 and S100A9 activate MAP kinase and NF-kappaB signaling pathways and trigger translocation of RAGE in human prostate cancer cells*. Exp. Cell. Res. **2006**, *312*, 184–197.

Hermani, A., Hess, J., De Servi, B., Medunjanin, S., Grobholz, R., Trojan, L., *et al.* (2005) *Calcium-binding proteins S100A8 and S100A9 as novel diagnostic markers in human prostate cancer.* Clin Cancer Res 2005;11(14):5146–52.

Ichikawa, M., Williams, R., Wang, L., Vogl, T. and Srikrishna, G. (2011) *S100A8/A9 activate key genes and pathways in colon tumor progression*. Mol. Cancer Res. **2011**, 9, 133–148.

Ishikawa, K., Nakagawa, A., Tanaka, I., Suzuki, M. and Nishihira, J. (2000) *The structure of human MRP8, a member of the S100 calcium-binding protein family, by MAD phasing at 1.9 A resolution*. Acta Crystallogr. Sect. D Biol. Crystallogr. **2000**, 56, 559–566.

Kang, J-H., Hwang, S-M. and Chung I-Y. (2014) *S100A8, S100A9 and S100A12 activate airway epithelial cells to produce MUC5AC via extracellular signal-regulated kinase and nuclear factor-jB pathways.* John Wiley & Sons Ltd, Immunology, 144, 79–90. doi:10.1111/imm.12352 Received 07 March 2014; revised 29 May 2014; accepted 25 June 2014.

Khan, F., Legler, P. M., Mease, R. M., Duncan, E. H., Bergmann-Leitner, E. S., and Angov, E. (2012) *Histidine affinity tags affect MSP1(42) struc- tural stability and immunodominance in mice*. Biotechnol. J. 7, 133–147. doi: 10.1002/biot.201100331

Klose, J., Wendt, N., Kubald, S., Krause, E., Fechner, K., Beyermann, M., *et al*. (2004). *Hexa-histidin tag position influences disulfide structure but not binding behavior of in vitro folded N-terminal domain of rat corticotropin-releasing factor receptor type 2a.* Protein Sci. 13, 2470–2475. doi: 10.1110/ps.04835904

Korndörfer, IP., Brueckner, F. and Skerra, A. (2007) *The crystal structure of the human (S100A8/S100A9)2 heterotetramer, calprotectin, illustrates how conformational changes of interacting a-helices can determine specific association of two EF-hand proteins.* J Mol Biol 2007; **370:** 887 – 898.

Korpimaki, T., Kurittu, J., and Karp, M. (2003) *Surprisingly fast disappearance of beta-lactam selection pressure in cultivation as detected with novel biosensing approaches*. J. Microbiol. Methods 53, 37–42. doi: 10.1016/S0167-7012(02) 00213-0

Kunsch, C. and Medford, RM. (1999) *Oxidative stress as a regulator of gene expression in the vasculature.* Circ Res 85: 753–766, 1999.

Lawrence, T., (2009) *The Nuclear Factor NF-κB Pathway in Inflammation*. Cold Spring Harbor Laboratory Press; all rights reserved; doi: 10.1101/cshperspect.a001651 Cite this article as Cold Spring Harb Perspect Biol 2009;1:a001651

Leukert N, vogl T, Strupat K, Reichelt R, Sorg C, Roth J (2006) *Calcium-dependent tetramer formation of S100A8 and S100A9 is essential for biological activity*. J Mol Biol 359(4):961–972. doi:10.1016/j.jmb.2006.04.009

Lim SY., Raftery, MJ., Goyette, J., Hsu, K. and Geczy, CL. (2009) *Oxidative modifications of S100 proteins: functional regulation by redox*. J Leukoc Biol 86: 577–587, 2009.

Lim, SY., Raftery, MJ. and Geczy, CL. (2011) *Oxidative modifications of DAMPs suppress inflammation: the case for S100A8 and S100A9.* Antioxid Redox Signal. 15: 2235–2248.

Loser, K., Vogl, T., Voskort, M., Lueken, A., Kupas, V., Nacken, W., Klenner, L., Kuhn, A., Foell, D., Sorokin, L., *et al*. (2010) *The Toll-like receptor 4 ligands Mrp8 and Mrp14 are crucial in the development of autoreactive CD8+ T cells.* Nat. Med. **2010**, 16, 713–717.

Manitz, M. P., Horst, B., Seeliger, S., Strey, A., Skryabin, BV., Gunzer, M., Frings, W., Schönlau, F., Roth, J., Sorg, C. and Nacken, W. (2003) *Loss of S100A9 (MRP14) results in reduced interleukin-8- induced CD11b surface expression, a polarized microfilament system, and diminished responsiveness to chemoattractants in vitro*. Mol. Cell Biol. 23, 1034–1043 (2003).

Medzhitov, R. and Janeway, CA Jr. (2002) *Decoding the patterns of self and nonself by the innate immune system*. Science 296: 298–300, 2002.

Mørk, G., Schjerven, H., Mangschau, L., Soyland, E. and Brandtzaeg, P. (2003) *Proinflammatory cytokines upregulate expression of calprotectin (L1 protein, MRP-8/MRP-14) in cultured human keratinocytes*. Br. J. Dermatol. **2003**, 149, 484–491.

Nagai, K. and Thogersen, HC. (1987) *Synthesis and sequence specific proteolysis of hybrid proteins produced in Escherichia coli.* Methods Enzymol 153:461–481

Narumi, K., Miyakawa, R., Ueda, R., Hashimoto, H., Yamamoto, Y., Yoshida, T. and Aoki, K. (2015) *Proinflammatory Proteins S100A8/S100A9 Activate NK Cells via interaction with RAGE*. J Immunol 2015; 194:5539-5548; Prepublished online 24 April 2015; doi: 10.4049/jimmunol.1402301

Qin, F., Song, Y., Li, Z., Zhao, L., Zhang, Y. and Geng, L. (2010) *S100A8/A9 Induces Apoptosis and Inhibits Metastasis of CasKi Human Cervical Cancer Cells.* Pathol. Oncol. Res. (2010) 16:353–360 DOI 10.1007/s12253-009-9225-2

Rammes, A., Roth, J., Goebeler, M., Klempt, M., Hartmann, M. and Sorg, C. (1997) *Myeloid-related protein (MRP) 8 and MRP14, calcium-binding proteins of the S100 family, are secreted by activated monocytes via a novel, tubulin- dependent pathway*. J. Biol. Chem. 272 (1997) 9496–9502.

Rosano, GL. and Ceccarelli, EA. (2014) *Recombinant protein expres- sion in Escherichia coli: advances and challenges.* Front. Microbiol. **5**:172. doi: 10.3389/fmicb.2014.00172

Ross KP and Herzberg MC. (2001) *Calprotectin expression by gingival epithelial cells.* Infect hmmn 2001: 69; J248-^4,

Ryckman, C., Vandal, K., Rouleau, P. *et al* (2003) *Proinflammatory activities of S100: proteins S100A8, S100A9, and S100A8/A9 induce neutrophil chemotaxis and adhesion*. J Immunol 170 (6):3233–3242

Shen, J., Person, MD., Zhu, J., Abbruzzese, JL. and Li, D. (2004) *Protein expression profiles in pancreatic adenocarcinoma compared with normal pancreatic tissue and tissue affected by pancreatitis as detected by two-dimensional gel electrophoresis and mass spectrometry.* Cancer Res 2004;64(24):9018–26.

Simard, J-C., Cesaro, A., Chapeton-Montes, J., Tardif, M., Antoine, F., Girard, D., and Tessier, P. A. (2013) *S100A8 and S100A9 Induce Cytokine Expression and Regulate the NLRP3 Inflammasome via ROS-*

Dependent Activation of NF-κB1. PLoS ONE, 8(8), e72138. doi:10.1371/journal.pone.0072138

Sinha, P., Okoro, C., Foell, D., Freeze, H.H., Ostrand-Rosenberg, S. and Srikrishna, G. (2008) *Proinflammatory S100 proteins regulate the accumulation of myeloid-derived suppressor cells.* J. Immunol. **2008**, 181, 4666–4675.

Strupat, K., Rogniaux, H., van Dorsselaer, A., Roth, J. and Vogl, T. (2000) *Calcium-induced noncovalently linked tetramers of MRP8 and MRP14 are confirmed by electrospray ionization-mass analysis.* J. Am. Soc. Mass Spectrom. **2000**, 11, 780–788

Terpe, K. (2002) *Overview of tag protein fusions: from molecular and biochemical fundamentals to commercial systems*. Appl Microbiol Biotechnol (2003) 60:523–533 DOI 10.1007/s00253-002-1158-6

van Beijnum JR., Buurman, WA. and Griffioen, AW. (2008) *Convergence and amplification of toll-like receptor (TLR) and receptor for advanced glycation end products (RAGE) signaling pathways via high mobility group B1 (HMGB1).* Angiogenesis. 11(1):91-9.

Vogl, T. (2010) Unpublished work. University of Muenster, Muenster, Germany.

Vogl, T., Gharibyan, A.L., and Morozova-Roche, L.A. (2012*). Pro-inflammatory S100A8 and S100A9 proteins: self-assembly into multifunctional native and amyloid complexes*. Int. J. Mol. Sci. *13*, 2893–2917.

Vogl, T., Leukert, N., Barczyk, K., Strupat, K. and Roth, J. (2006) *Biophysical characterization of S100A8 and S100A9 in the absence and presence of bivalent cations.* Biochim. Biophys. Acta 1763: 1298–1306.

Vogl, T., Ludwig, S., Goebeler, M., Strey, A., Thorey, I.S., Reichelt, R., Foell, D., Gerke, V., Manitz, M.P., Nacken, W. *et al*. (2004) *MRP8 and MRP14 control microtubule reorganization during transendothelial migration of phagocytes.* Blood 2004, *104*, 4260–4268.

Vogl, T., Tenbrock, K., Ludwig, S., Leukert, N., Ehrhardt, C., van Zoelen, M.A., Nacken, W., Foell, D., van der Poll, T., Sorg, C. *et al*. (2007) *Mrp8 and Mrp14 are endogenous activators of Toll-like receptor 4, promoting lethal, endotoxin-induced shock.* Nat. Med. 2007, 13, 1042–1049.

Wu, J. and Filutowicz, M. (1999) *Hexahistidine (His6)-tag dependent protein dimerization: a cautionary tale.* Acta Biochim Pol 46:591–599

Yamagishi S-I., Matsui, T. and Fukami, K. (2015) *Role of Receptor for Advanced Glycation End Products (RAGE) and Its Ligands in Cancer Risk*. REJUVENATION RESEARCH Volume 18, Number 1, 2015 a Mary Ann Liebert, Inc. DOI: 10.1089/rej.2014.1625

Yang, Z., Zhang, L., Zhang, Y., Zhang, T., Feng, Y., Lu, X., Lan, W., Wang, J., Wu, H., Cao, C. and Wang, X. (2011) *Highly efficient production of soluble proteins from insoluble inclusion bodies by a two-step-denaturing and refolding method*. PloS one 6.7 (2011): e22981.

Zhang, J.-M., & An, J. (2007) *Cytokines, Inflammation and Pain*. International Anesthesiology Clinics, 45(2), 27–37. doi:10.1097/AIA.0b013e318034194e

Appendix

Appendix I: A detailed version of the pET-45b vector containing a human S100A8 cDNA cloned and inserted in the *Kpn*I and *Pac*I sites of the vector. The vector also contains cDNA of the enterokinase recognition site and cDNA of six histidines.

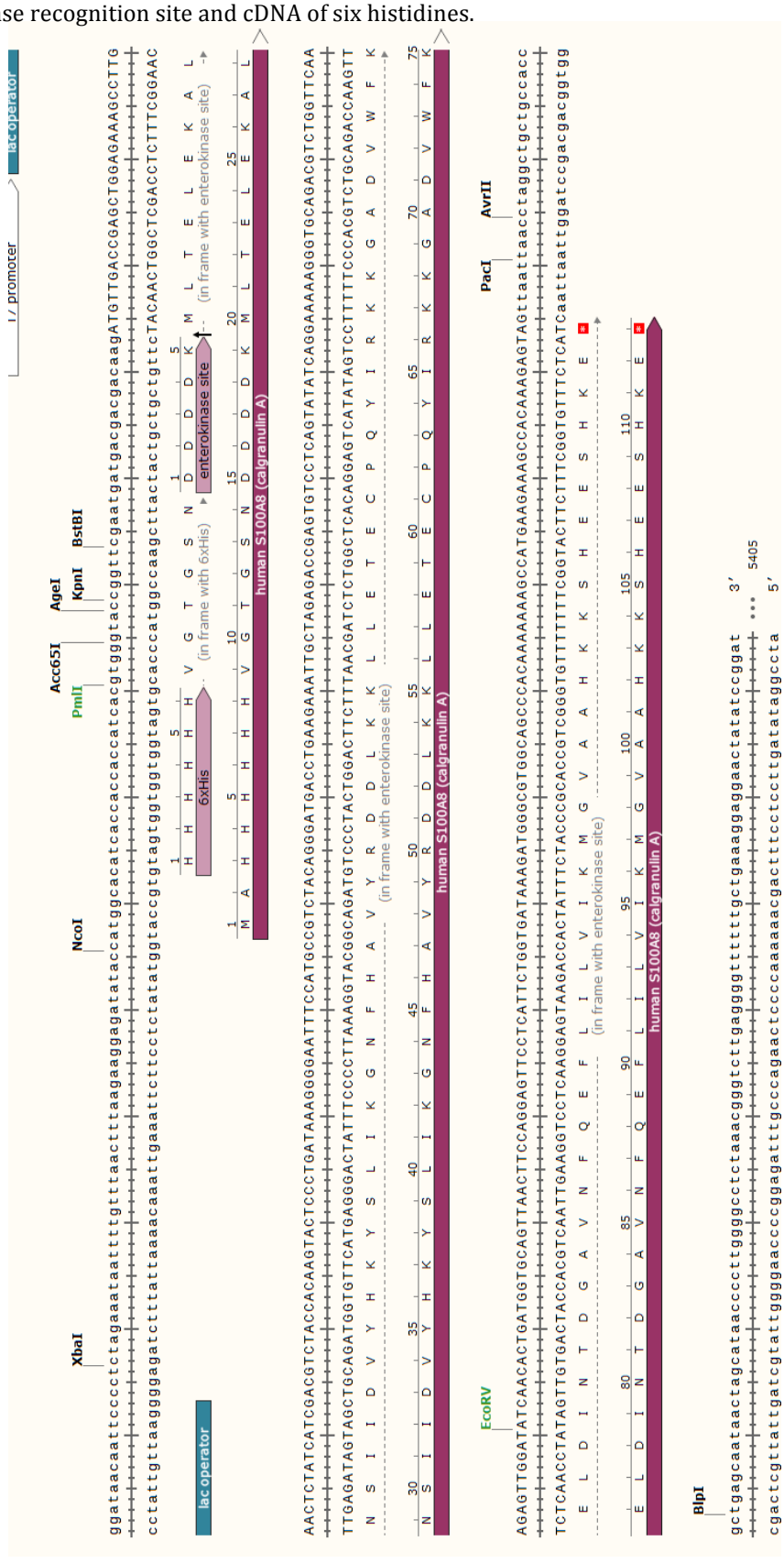

Appendix II: Western blot analysis of samples before and after the purification step with size-exclusion chromatography on a Superdex 75 11/790 column. The sample containing protein solution before the column is shown a clear band above 10 kDA MWM, whereas samples after the column are not visible. This verifies that there were proteins prior to the column but has disappeared after the column due to fragmentation or protein loss.

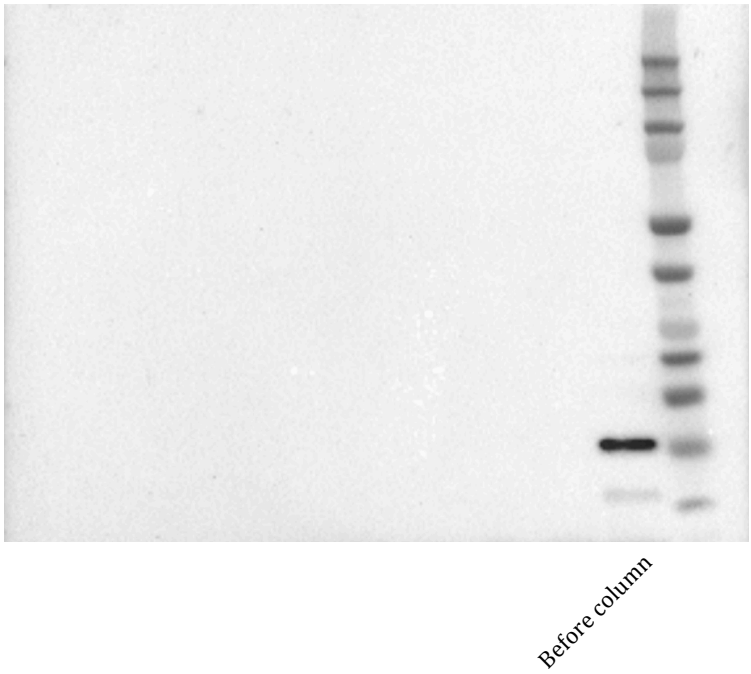

Appendix III: SDS-PAGE analysis of the fractions collected after the purification step with anion-exchange chromatography on a HiPrep Q FF 16/10 column. Fraction 17 shows strongest bands with equal amounts of wt-S100A8 and wt-S100A9 and closest to homogeneity, hence it was were collected for further experiments

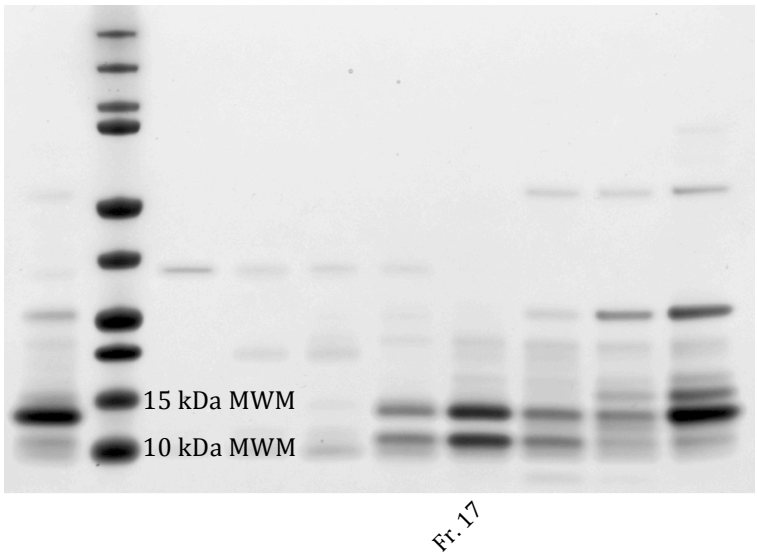

Appendix IV: Purity of His_6-rhS100A8 (13 kDa) analysed with SDS-PAGE.

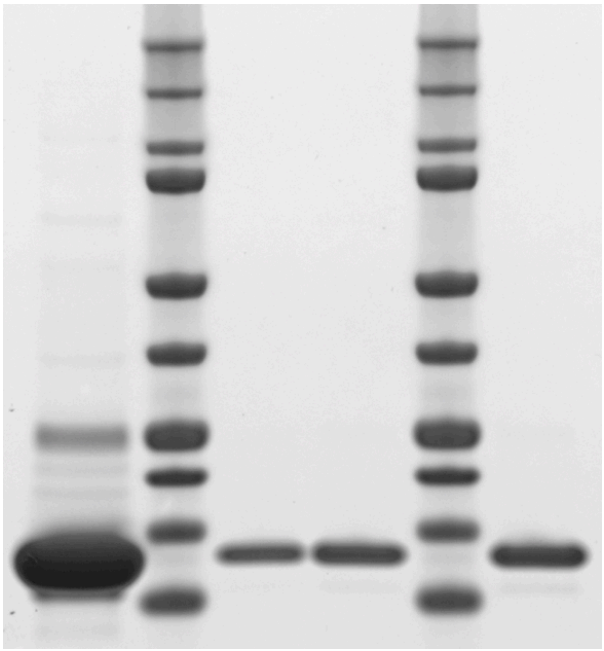

Appendix V: LC-MS chromatogram of wt-rhS100A9. The exact mass was determined to 13112 compared to the theoretically calculated mass of 13110 Da.